PRELIMINARY EXPLORATION PROGRAM REPORT FOR CASSITERITE IN TULU AREA, BAUCHI STATE, NIGERIA

DMW LOVOL ENGINEERING LTD.

OCTOBER 2, 2025

DMW LOVOL ENGINEERING LTD.
12B, Mabinuori Dawodu St, Charly Boy Bus-Stop, Gbagada Phase 1, Lagos, Nigeria.

TABLE OF CONTENTS

TABLE OF FIGURES

EXECUTIVE SUMMARY

1. DMW LOVOL Engineering Limited is a natural resources company engaged in the exploration and development of mineral properties. The company is currently focused on an early-stage cassiterite exploration project located in the highly prospective region of Bauchi, Nigeria, with the current project situated in the Tulu area of Bauchi, Nigeria. The primary objectives of this exploration program were to conduct initial geological mapping to identify key rock types and structural features within the license area, and to perform systematic soil sampling from carefully excavated pits to obtain representative material from specific depths. All soil and rock samples were then analyzed geochemically to determine their elemental concentrations and to evaluate the presence of tin mineralization. The results were assessed to understand the spatial and vertical distribution of anomalies and, where possible, linked to the underlying geology. These findings were used to establish a clear protocol to guide the next phase of exploration.

   This report summarizes the first phase of cassiterite (tin ore) exploration carried out by DMW LOVOL Engineering Ltd. over its 40 km^2 licensed area in the Tulu region of Bauchi State, Nigeria. The work involved detailed geological mapping, systematic pitting, and laboratory analysis of both rock and soil samples. The primary objective was to determine the distribution of tin dioxide (SnO_2) across the license area and with depth, using cutoff grades of 0.3% for rock samples and 0.2% for pit samples.

2. The exploration program applied a combination of methods, including remote sensing, geological mapping, and a pitting program involving both soil and stream channel sampling. The collected samples were then subjected to standard preparation procedures, followed by geochemical analysis using X-ray Fluorescence (XRF) and X-ray Diffraction (XRD) techniques, all aimed at evaluating the cassiterite potential within the licensed area.

   Remote sensing was applied to obtain a regional overview of the license area and to identify surface features and structural trends that may influence mineralization. These results were refined through detailed geological mapping on a scale of 1:25,000, which focused on delineating rock types, intrusive contacts, and structural features such as faults and joints. Mapping also provided ground verification of anomalies detected through remote sensing and highlighted features known to control cassiterite mineralization in the Younger Granite Province.

   A systematic pitting program was undertaken to obtain representative samples from both soils and stream channels. A total of 188 pits (410.1m) were excavated within the licensed area. Soil samples were collected from excavated pits at four (4) depth intervals (0-0.3m, 0.3-1m, 1-2m, >2m) to capture the vertical distribution of geochemical signatures in the regolith. Stream channel sampling was conducted to assess the secondary dispersion patterns of cassiterite and associated minerals within drainage systems. This dual approach provided complementary datasets, enabling more reliable identification of anomalous zones.

   Soil, stream, and rock samples collected during the pitting and geological mapping program underwent sample preparation to ensure quality and integrity. Soil and stream samples were first cleaned of debris, air-dried in sterile polyethylene sheets, homogenized, and ground using chemically inert porcelain mortars before being sieved to 63 microns. The fine fractions were sealed in resealable sachets for laboratory analysis, with nineteen duplicates prepared as part of the quality assurance process. Rock samples were processed at the Mineral Processing Unit of the NMDC in Jos, where they were crushed using a jaw crusher, milled into fine powders with a ring and puck mill, and packaged in ziplock bags. All preparation steps involved careful cleaning of equipment with methylated spirits to prevent cross-contamination. Additional petrographic work involved cutting rock blocks with safety-compliant grinding and cutting procedures.

Following preparation, the pulverized samples (63 microns) were sealed in correctly numbered plastic bags and submitted to the National Steel Raw Materials Exploration Agency (NSRMEA) in Kaduna. Each pit interval was entered under a single submission number, with sample weights recorded and packed into larger batches for transport. Before dispatch, samples were stored securely at the DMW LOVOL exploration office in Jos, located within a gated compound to ensure restricted access. Transportation to NSRMEA was carried out in independently operated vehicles by DMW LOVOL geologists under the supervision of senior staff, ensuring secure handling from the site to the laboratory.

Collected samples were prepared using standard laboratory protocols to ensure accuracy and consistency.

Geochemical analysis was then conducted on both rock and soil samples using X-ray Fluorescence (XRF), which provided quantitative measurements of elemental concentrations. Particular attention was given to tin and associated pathfinder elements, as these are critical indicators of cassiterite mineralization. The XRF data formed the basis for assessing geochemical anomalies across the project area.

In addition to elemental analysis, mineralogical characterization was carried out on the rock samples using X-ray Diffraction (XRD). This technique was used to identify crystalline phases within the samples and to confirm the presence of cassiterite where possible. XRD complemented the XRF results by providing mineral-level confirmation of geochemical anomalies, thereby strengthening the overall interpretation of mineralization potential.

3. The license area is made up mainly of silica-rich granites of the Younger Granite province intruding the Basement Complex. These rocks are dominated by quartz, feldspars, and muscovite, with several samples showing high muscovite content and greisen alteration, both of which are strong indicators of tin-bearing systems. The presence of greisenized granites, muscovite-rich monzogranites, and the overall peraluminous nature of the granitoids point to highly fractionated magmas and late-stage fluid activity, the exact geological conditions needed for cassiterite mineralization. In simple terms, the rocks in this area belong to the same tin-rich granite lineage that has made the Jos Plateau world famous, and the mineral and alteration features we see here strongly support the area's potential to host significant cassiterite deposits.

   The integrated geochemical results from soil Intervals A–D confirm that cassiterite mineralization within the Younger Granite Complex is vertically extensive, with anomalies present from surface to deep horizons. Using a 0.2% SnO_2 cutoff, anomalous samples account for 8.6% in Interval A, 9.3% in Interval B, 8.7% in Interval C, and the highest frequency of 10.6% in Interval D. Grades range from background levels up to 1.96% SnO_2 (Interval B), with additional significant anomalies including 0.85% in Interval A, 0.51% in Interval C, and 0.74% in Interval D, confirming continuity of tin enrichment across the soil profile. Correlation analysis shows that SnO_2 is consistently and positively associated with zircon (ZrO_2) and tantalum oxides (Ta_2O_5), making these the most reliable pathfinders. At the same time, Fe_2O_3 exhibits strong negative correlations and P_2O_5 shows weak to negative associations, indicating that ferruginization and phosphate enrichment are not dependable guides to cassiterite. TiO_2 and Nb_2O_5 display weak positive trends and are of secondary importance. Overall, the geochemical evidence demonstrates a deep residual cassiterite system with zircon and tantalum as key companion minerals, justifying further trenching, bulk sampling, and heavy mineral analysis to delineate ore-bearing zones.

The geological mapping and analysis of 47 rock samples confirm widespread cassiterite mineralization within the license, with 59.1% of samples exceeding the 0.30% SnO_2 cutoff and grades reaching up to 0.96%. High tin values are concentrated in areas such as Gurungu and Estoyaki, with additional significant anomalies at Bangotama, Tulu, Lemoro, Wulkai, Maje Uku, and Ba Karpa. Anomalous samples occur across a range of granitoids including syenogranite, granodiorite, quartzolite, and monzogranite, as well as muscovite-rich and greisenized rocks, highlighting the peraluminous and fluid-altered character of the intrusives. Chemically, cassiterite enrichment is marked by lower Fe_2O_3, higher ZrO_2 and Nb_2O_5, and a weak positive link with Ta_2O_5, while iron and phosphorus show negative associations. This geochemical and spatial pattern is typical of the Younger Granite province, where dispersed, low- to medium-grade tin in bedrock serves as the primary source for secondary placer and residual deposits, underscoring the strong potential of the area to host significant cassiterite resources.

The XRD study of 47 rock samples from the licensed area reveals that the bedrock is dominated by quartz-rich, peraluminous granitoids—granites, monzogranites, syenogranites, and greisenized intrusives, characterized by high quartz (40–70%), alkali and plagioclase feldspars, and abundant muscovite in some cases. These mineralogical fingerprints align with the classic tin granite lineage of the Jos Younger Granite province, where muscovite enrichment and greisen alteration signal strong fluid–rock interaction, a key driver of cassiterite mineralization. Although cassiterite (SnO_2) was not detected by XRD due to its low modal abundance and fine-grained occurrence, the host rock assemblages and alteration textures provide compelling evidence of a fertile magmatic system. Taken together with geochemical assays, these results confirm that the area has the right geological and petrogenetic conditions for cassiterite, and exploration should prioritize greisenized zones, muscovite-rich granites, and quartz-rich veins as prime tin targets.

4. The results are highly encouraging. Several rock samples returned values above the 0.3% cutoff, with some as high as 0.74% SnO_2. This indicates that the bedrock beneath the area hosts primary tin mineralization, the source of the cassiterite. The pitting program, which involved digging 188 pits and sampling at four depth intervals (from surface down to more than 2 meters), produced very positive results. Thirty-two pit samples exceeded the 0.2% cutoff, with standout values of 1.96% SnO_2 in pit DMW-126, 0.55% in DMW-038, and 0.51% in DMW-533. These high-grade results are concentrated in specific areas, rather than being evenly spread out, indicating zones of strong mineral potential. Importantly, the higher tin values are not limited to surface soils but extend deeper, in some cases even increasing at depths of 1–2 meters and below. This suggests that the mineralization is not just a shallow

surface occurrence but a more robust and persistent deposit, possibly residual or deep alluvial in nature. This is a key sign of a potentially significant and commercially viable resource. When compared to other tin deposits, the findings from Tulu are very favorable. The geological setting matches well with Nigeria's Younger Granites, which have historically supplied over 95% of the country's tin. Although the grades are not as high as Bolivia's world-class lode deposits (over 4.7% Sn metal), they are far above the global average for alluvial deposits (0.01% Sn metal). For this type of deposit, the results are considered excellent.

5. The recommended next steps for the project include focused infill pitting and trenching to better outline the size and shape of the mineralized zones, metallurgical testing through heavy mineral separation to determine the recoverable cassiterite concentrate and assess economic viability, and exploratory drilling to investigate deeper tin sources such as buried channels or concealed primary lodes. In summary, the Tulu project has shown very strong potential for a commercial cassiterite resource, and the combination of favorable geology with promising geochemical results provides a solid foundation for advancing to more detailed exploration.

CHAPTER ONE

1.0 PROJECT CONTEXT AND FRAMEWORK

DMW LOVOL Engineering Limited, a diversified resource company, initiated various stages of exploration projects to evaluate the potential for Cassiterite (Tin) mineralization in its project area, located in Tulu, Toro Local Government Area, Bauchi State. Toro LGA is one of the areas with high potential for tin ore deposits in Nigeria.

This report enunciates a work program for detailed exploration activities to assess the presence and extent of tin, columbite, and monazite (TCM) deposits within the EL of the company stated above. The project area, located approximately 30 km from Toro town, is geologically situated within the basement complex. Exploration activities to date comprised a combination of remote sensing, aeromagnetic surveys, geochemical sampling, and minimum work programs in some parts of the area. The work program aims to identify mineralization zones by conducting a grid-by-grid soil sampling (pitting) of the project area.

Field observations were duly recorded, and the description of geological structures matched the pre-existing geological reports for the project area. Soil and stream sediments were subjected to standard scientific procedures and measures right from the field until they were sent to reputable institutions for geochemical analysis.

1.1 Strategic Objectives of the Program

The DMW team explored the areas within the company's license, covering 200 Cadaster Units (CUs) around the Tulu area in Bauchi State, for the occurrence of tin mineralization. This report presents the preliminary findings from the exploration activities.

The principal objectives of this exploration program were:

- To conduct initial geological mapping to identify the principal rock types and structures within the license area.
- To execute a systematic soil sampling from excavated pits to collect representative samples of the soil and regolith at predetermined depths.
- To undertake geochemical analysis of all the samples (rocks and soils) to determine the elemental concentration
- To ascertain whether the samples bear evidence of tin mineralization
- To interpret the spatial and vertical distribution of these anomalies, correlating them with geological features where possible.
- To develop an appropriate protocol for the subsequent exploration phase.

1.2 Property Description and Location

The Project area is located within the Toro Local Government Area of Bauchi State, with Exploration License number EL-44923. The property is near Tulu village, approximately 30 km northwest of Toro Local Government Area. It consists of 200 cadastral units (200CU) covering a 40 Km2 area (Figure) and is situated within Longitude $8^{0}52'30''$ E – $9^{0}07'30''$ E and Latitude

10^{0}28’45” N – 10^{0}43’45” N. The hosting communities are Tulu, Bangontama, and Gurungu. It falls within the Younger Granite Suite and the Older Granites of Nigeria basement complex, and is accessible via a matrix of tarred road network, unpaved roads, and footpaths. The boundary coordinates of the Exploration Licenses are tabulated below.

Table 1: The Corner coordinates of the project area

08° 59' 00" E	10° 33' 45" N
09° 01' 30" E	10° 33' 45" N
09° 01' 30" E	10° 38' 45" N
08° 59' 00" E	10° 38' 45" N

1.3 Ownership

The tenement is registered in and owned by DMW LOVOL Engineering Limited. The Project area, located within the Toro Local Government Area of Bauchi State, bears the Exploration License number EL-44923.

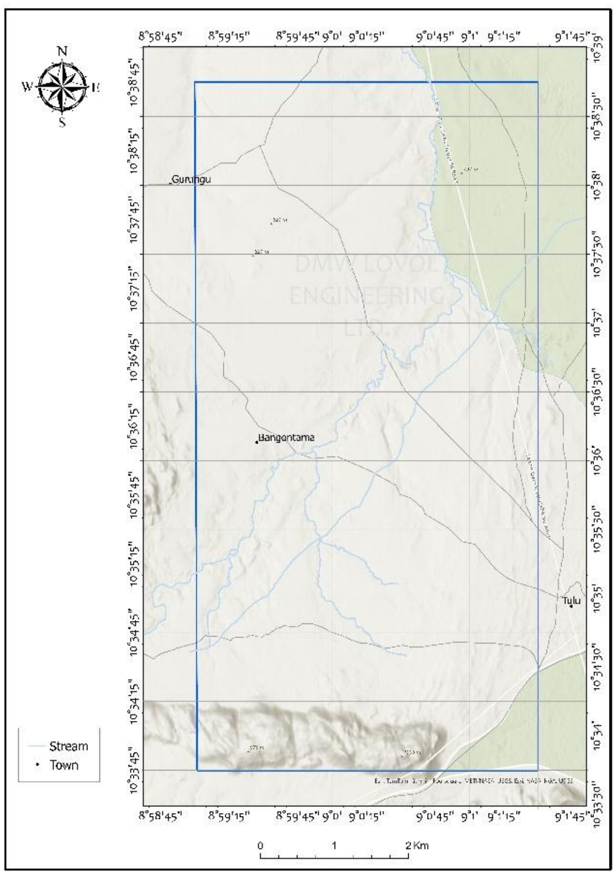

Figure 1 The DMW Tulu Project area Area

1.4 Accessibility, Topography, and Climate

It is worth reiterating that the project area is situated in Toro Local Government, Bauchi State, Nigeria. Toro Local Government Area is often regarded as the most populous local government area in Nigeria and West Africa. It shares a boundary with Plateau, Kaduna, and Kano states. It boasts a population of about 1.2 million people. Most of whom are subsistence farmers and small-scale business people.

The project area is accessible via the Magaman Gumau - Saminaka road and a network of unpaved roads that link to other villages within the community. The streets are better traversed during the dry season, as flooding can make the town inaccessible during the rainy season. The area has an undulating topography with an elevation range of 777m to 863m, and is fairly drained, with perennial rivers that serve as minor tributaries of the main rivers. A dendritic drainage pattern characterizes it. Most streams in the area get recharged during the rainy season. The area is characterized by two distinctive seasons, the rainy season and the dry season. Rainfall in the state is highly irregular in space and time. This makes farming somewhat challenging, as slight differences in the amount and timing of rain received at a site can determine the success or failure of critical stages in vegetation development and crop production.

Rain typically commences from around April until between August and September, with levels ranging from 760 mm to 1051 mm. The rainfall sometimes produces hailstorms.

Bauchi experiences an oppressive wet season, while the dry season is partly cloudy, and temperatures remain hot year-round. Over the year, the temperature also varies. Nevertheless, the mean daily temperature could be as low as 20°C during December and January when the cold, dry Harmattan wind blows from the Sahara Desert.

1.5 Vegetation

Bauchi state is one of the states in the northern part of Nigeria that span two distinctive vegetation zones, namely, the Sudan savannah and the Sahel Savannah.

Toro Local Government Area in Bauchi state, Nigeria, is located within the Sudan Savannah ecological zone. This influences its vegetation. This area is characterized by a mixture of savanna vegetation and semi-arid features, transitioning between the Sahel in the north and the Guinea savanna in the south.

1.6 Status of Exploration, Development, and Operations

The project is still within its exploration stage as licensed by the Federal Ministry of Mines and Steel Development, Nigeria. There has been no official report from the Federal Ministry of Mines and Steel Development, Bauchi, Nigeria, about any illegal practices observed after the issuance of the license.

A total of 28 soil samples were initially collected during the reconnaissance survey conducted by the Geology Department of DMW LOVOL Engineering from May 10 to 19, 2023. The samples collected were subjected to geochemical analysis to evaluate their mineral content.

Following this, a geophysical survey was conducted in April 2023 to identify geological structures, assess the area's physiography, and understand the depositional environment and its geological and mineralization context.

On April 14, 2025, the company's geology department commenced a rigorous soil sample collection from both stream channels and the surrounding soil. This exercise was accompanied by geological mapping to further understand the geology of the project area.

As of the time of this report, about five hundred and seventeen nine stream sediments and soil samples were obtained and prepared for analysis. Rock samples obtained were also pulverized and sent for analysis.

1.6 Geological Setting: The Younger Granite Province of Nigeria

The DMW Tulu license is situated within the well-established Younger Granites province of Nigeria. This province is a classic example of Mesozoic anorogenic magmatism, where a suite of high-level, magmatic granitic masses discordantly intrudes the older Precambrian Basement Complex.[2] This igneous activity resulted in the formation of distinctive ring-dyke complexes and extensive, high-relief plateaus, which are prominent topographic features in the region [4]

The Younger Granites are particularly renowned for their association with tin and niobium mineralization.[5] The primary tin mineralization is confined almost exclusively to biotite granites and occurs in two primary forms: disseminations within albitized granites and as greisen lodes and veins.[2] The tin found in the alluvial deposits is believed to have originated from these primary sources.[2] Historically, this type of mineralization has been the engine of Nigeria's tin production, with over 95% of the total cassiterite output having been won from alluvial and residual deposits derived from the tin-bearing Younger Granites and associated lodes.[2] Cassiterite mineralization typically occurs as both primary lode deposits within greisenized granites and quartz veins, as well as secondary placer deposits concentrated along stream channels. The Tulu project area, therefore, lies within a proven metallogenic setting, providing a strong geological foundation for the current exploration program.

CHAPTER TWO

2.0 WORK CARRIED OUT DURING REPORTING PERIOD

2.1 Geological Mapping

Geological mapping of the licensed area was undertaken at a scale of 1:25,000, ensuring systematic coverage of the entire concession. This scale was selected as it provides an appropriate balance between regional coverage and sufficient detail to delineate lithological boundaries and structural features relevant to mineral exploration. It allows for an accurate depiction of central geological units while capturing the finer-scale structures that may exert control on mineralization.

The principal objective of the program was to establish the lithological and structural framework of the area. Mapping was executed along traverses designed to achieve uniform spatial distribution, with traverse orientations adjusted according to topography and accessibility.

Field procedures included detailed observation and recording of lithological contacts, textural and mineralogical characteristics of exposed outcrops, and the orientation of structural elements such as foliation, joints, faults, and vein systems. Measurements were acquired using standard geological field instruments, including compasses, clinometers, and handheld GPS units, to ensure positional and structural accuracy. Outcrop sketches, photographic records, and systematic field notes were compiled to supplement direct observations.

Representative sampling was integrated into the mapping program, with 43 samples collected across the concession. Sampling targeted fresh and weathered exposures of major lithological units, mineralized zones, and structurally controlled features to provide material suitable for geochemical characterization. Each sample location was precisely georeferenced to allow subsequent spatial correlation with mapped features.

The mapping methodology thus generated a comprehensive lithological and structural dataset, establishing a robust geological baseline upon which geochemical analyses and subsequent exploration phases can be reliably integrated.

2.2 Pitting Program

A total of 188 exploration pits were excavated across the licensed area as part of the surface geochemical investigation. The pits were positioned on a systematic grid at 250m and 450m intervals for the soil samples and 25m and 100m for the stream channel samples, providing uniform coverage of the concession and ensuring that both soil and regolith profiles were adequately represented. This approach enabled the collection of surficial material, including soils and stream sediments, while also exposing the weathering profile for direct geological observation.

Each pit was logged in detail, parameters recorded included horizon thickness, soil texture and color, lithological variations, and any observed evidence of mineralization or structural features. This information was supplemented with photographic records and GPS georeferencing to ensure spatial accuracy and data consistency.

Sampling within the pits was conducted at four depth intervals designed to characterize vertical geochemical variation within the profile:

- **Interval A:** 0–0.3 m (topsoil/surface layer)
- **Interval B:** 0.3–1.0 m (subsoil layer)
- **Interval C:** 1.0–2.0 m (deeper regolith/saprolite)
- **Interval D:** >2.0 m (basal regolith/saprolite)

This multi-layered sampling strategy provided insight into both surface dispersion patterns and the potential for in-situ cassiterite concentration within the weathering profile.

Rigorous QA/QC protocols were applied throughout the pitting program to ensure reliability and reproducibility of results. Duplicate samples were collected at predefined intervals, while blank samples and certified reference materials (CRMs) were inserted into the sample stream to monitor laboratory accuracy and precision. Field instruments, including GPS units and measuring devices, were regularly calibrated, and all sampling tools were thoroughly cleaned between uses to minimize contamination.

Daily field audits were conducted to verify that pit logs matched GPS coordinates and sample tags. Any inconsistencies identified during these reviews were corrected immediately to maintain data integrity. The systematic application of QA/QC protocols ensured that the dataset generated from the pitting program met accepted industry standards and could be confidently integrated with subsequent geochemical analyses.

2.3 Sample Preparation

The following procedure details the systematic preparation of soil, stream, and rock samples collected during the pitting and geological mapping exercise.

2.3.1 Soil and stream samples preparation

Unwanted materials, such as debris of sticks and leaves, were removed from the collected soil and stream samples. The samples were then thinly spread on a sterile polyethylene bag and evenly air-dried to prevent the loss of volatile components and avoid altering mineralogy, in a dust-free environment. Large clumps in the dried samples were broken apart and thoroughly mixed to ensure homogeneity. The samples were ground to a fine powder using a porcelain mortar and pestle because of its chemical inertness. The finely ground samples were sieved through a 63-micron nylon mesh. The fine-grained samples were then stored and packaged in small resealable sachets in preparation for laboratory analysis. A total of nineteen (19) samples were duplicated for quality assurance and to verify the integrity of the analytical machine. The mortar and pestle were cleaned intermittently with methylated spirits, while clogged particles in the sieve mesh were gently removed using a brush to prevent any cross-contamination.

2.3.2 Rock samples preparation

Chemical and Structural analysis

The rock samples were prepared at the Mineral Processing Unit of the National Metallurgical Development Centre (NMDC), Jos. The rock samples were disaggregated with a jaw crusher. The disaggregated samples were then further broken down into smaller pieces using a mortar and pestle. The samples were ground into a fine powder with a ring and puck mill and packaged in Ziplock bags. The ring and puck mill were thoroughly cleaned with methylated spirits and wool after each sample preparation to prevent cross-contamination.

Petrographic Analysis

The rock samples were cut into blocks using a grinder and granite cutting blades. Safety precautions were followed during the cutting process by wearing personal protective equipment (PPE), such as safety glasses, hearing protection, and gloves.

2.3.3 Sample Dispatch

The rock and soil samples were submitted to the National Steel Raw Materials Exploration Agency (NSRMEA) laboratory in Kaduna as pulverized material, prepared to a 63-micron size, and sealed in correctly numbered plastic bags. Standard procedures developed and documented by DMW geologists were strictly followed. At the field site, all samples from each hole were separated based on interval and entered under a single submission form, ensuring that each hole interval carried only one submission number. Individual sample weights were carefully recorded and then packed into large ziplock bags for ease of handling. DMW LOVOL geologists subsequently transported the complete sample batch to the NSRMEA laboratory for further analysis.

2.3.4 Sample Security

Prior to dispatch, all samples were securely stored at the DMW LOVOL exploration office in Jos. The office and sampling facilities are situated within a single, walled compound with a gated entrance, ensuring controlled access and security. For transportation, the samples were carefully packed onto an independently owned and operated vehicle by DMW LOVOL geologists and driver under the direct supervision of senior geological staff, and delivered directly to NSRMEA in Kaduna for onward analysis.

2.4 Analytical Methods

A total of 47 rock samples and 583 pit samples were subjected to laboratory analysis using X-ray Fluorescence (XRF) to determine their bulk chemical composition, with particular emphasis on tin oxide (SnO_2) concentrations. In parallel, X-ray Diffraction (XRD) analysis was conducted on the 47 rock samples to determine the modal mineralogy and identify the mineral phases present. These complementary techniques provide both geochemical and mineralogical datasets that form the basis for interpretation.

2.4.1 Geochemical Analysis (XRF)

A total of 630 samples, comprising 47 rock samples and 583 soil samples, were submitted for geochemical analysis. The objective of this program was to establish the elemental composition of surface and bedrock materials, with particular emphasis on elements indicative of cassiterite mineralization and associated pathfinders. Analytical work was conducted by the National Steel Raw Materials Exploration Agency (NSRMEA), Kaduna, Nigeria, which operates accredited laboratories and employs internationally recognized procedures for sample preparation and analysis. All samples were catalogued and assigned unique identification numbers before dispatch. Strict cleaning protocols were observed between successive samples to minimize the risk of cross-contamination.

Geochemical analysis was conducted using X-Ray Fluorescence (XRF) Spectrometry, a non-destructive technique widely employed in mineral exploration for its precision in detecting major, minor, and selected trace elements. In this method, prepared powdered samples were pressed into pellets using a hydraulic press.

To ensure reliability and reproducibility of results, rigorous QA/QC measures were integrated into the geochemical program. Out of the 630 samples submitted, 19 samples were designated as QA/QC controls. These QA/QC samples were indistinguishable from routine samples in the batch sequence, ensuring unbiased assessment of laboratory performance. The application of XRF analysis, combined with a robust QA/QC protocol, generated a high-quality geochemical dataset. This dataset provides a reliable basis for interpreting elemental distribution patterns, establishing geochemical anomalies, and supporting ongoing exploration targeting within the licensed area.

2.4.2 Mineralogical Analysis

Thin Section

In addition to geochemical investigations, petrographic analysis was undertaken to provide a detailed understanding of the mineralogical and textural characteristics of rock samples from the licensed area. A total of 43 rock samples were submitted to the Department of Geology at the University of Ibadan, where they were processed into standard thin sections and examined under transmitted light microscopy.

The petrographic study aims to provide direct mineralogical evidence that complements geological mapping and geochemical analysis. By examining thin sections, the paragenetic sequence of minerals and the nature of mineral associations could be better understood. This is particularly relevant in evaluating the role of the Younger Granites and associated hydrothermal processes in the concentration of cassiterite and related mineralization.

Furthermore, petrographic data serve as a diagnostic tool for differentiating between lithological units that may appear similar in the field but exhibit distinct mineralogical or textural characteristics under the microscope. Such information strengthens the lithological framework established during mapping and provides a more robust foundation for exploration targeting.

X-ray Diffraction (XRD)

To complement the petrographic and geochemical investigations, 47 pulverized rock samples were submitted to the National Steel Raw Materials Exploration Agency (NSRMEA) in Kaduna for X-ray Diffraction (XRD) analysis. The objective of this program was to determine the precise mineralogical composition of the rocks, with particular attention to ore minerals, alteration products, and accessory phases that may not be easily distinguishable through field observation or optical microscopy alone.

Rock samples were first pulverized to fine powders to achieve a uniform grain size suitable for XRD analysis, typically less than 65 µm. Powdering ensures random orientation of mineral grains, which is critical for generating representative diffraction patterns. The powdered samples were then packed into holders and mounted in the diffractometer for analysis.

XRD analysis was conducted using a standard powder diffractometer. The pulverized fractions for various samples were analyzed using a Rigaku Miniflex 600 XRD instrument, employing Cu-Kα radiation at a 2θ angle of 2°–70 °. The XRD analysis provided critical mineralogical confirmation that complements thin section petrography and XRF geochemical results. Whereas thin section analysis is qualitative and reliant on optical properties, XRD offers quantitative identification of crystalline phases, including fine-grained or cryptocrystalline minerals that may be overlooked under the microscope.

This method is significant for characterizing alteration assemblages associated with mineralization, such as kaolinite, sericite, or chlorite, which serve as indicators of hydrothermal processes. In the context of tin exploration, XRD also helps confirm the presence of cassiterite and distinguish it from visually similar phases.

By integrating XRD results with petrographic and geochemical datasets, a more complete understanding of the lithological and alteration framework of the licensed area is achieved, thereby refining exploration models and supporting targeted follow-up work.

CHAPTER THREE

3.0 RESULTS OF INVESTIGATIONS

3.1 Geology of the Area (Based on the XRD results)

The XRD analyses of 47 pulverized rock samples confirm that the licensed area is underlain predominantly by felsic, silica-rich intrusive rocks belonging to the Younger Granite province of Nigeria, intruding into the Precambrian Basement Complex. The mineralogical assemblages identified are dominated by Quartz, Feldspars (Albite, Orthoclase, Microcline, Sanidine), and Micas (Muscovite, Phlogopite). These mineral modes classify the rocks mainly as Granites, Syenogranites, Monzogranites, and related granitoids.

Lithological Characteristics

1. **Granitoid Suite:**
    - High proportions of Quartz (40–70%) indicate that the intrusives are highly evolved felsic magmas.
    - Alkali feldspars (Orthoclase, Microcline, Sanidine) and sodic plagioclase (Albite) dominate, consistent with peraluminous granitic compositions.
2. **Muscovite-rich Rocks:**
    - Several samples contain significant Muscovite (up to ~44%), indicating peraluminous and fluid-rich compositions, a hallmark of tin-bearing granites.
    - Muscovite-bearing Monzogranites and Greisenized rocks suggest hydrothermal alteration linked to late-stage magmatic fluids.
3. **Greisenized and Altered Granites:**
    - Evidence of feldspar breakdown and replacement by quartz and muscovite highlights hydrothermal processes within the intrusives.
    - Such greisenization is strongly associated with cassiterite mineralization systems in the Younger Granites.

Geological Implications

- The dominance of silica-rich, peraluminous granites places the licensed area within the classical tin granite lineage. These granitoids represent highly fractionated magmas that are capable of concentrating rare metals, such as tin (Sn), niobium (Nb), tantalum (Ta), and tungsten (W).
- The identification of greisenized zones and muscovite-rich granites suggests that the area has undergone significant fluid–rock interaction, creating favorable conditions for cassiterite precipitation.
- The mineralogical framework is consistent with the broader geological model of the Jos Plateau Younger Granites, which are globally recognized for their tin–niobium–tantalum metallogeny.

In summary, the geology of the licensed area is characterized by evolved, peraluminous granitoids of the Younger Granite suite, which intrude into the Precambrian Basement. The presence of quartz-rich granites, muscovite-bearing granites, and greisenized intrusives confirms a geological environment highly prospective for cassiterite mineralization. These features collectively demonstrate that the concession lies within a fertile tin-bearing granite province, aligning with the regional metallogenic framework of central Nigeria.

3.2 Mineralogy of the rock Units

3.2.1 Rock Samples - XRD

The XRD analyses of 47 pulverized rock samples conducted at NSRMEA provided a detailed mineralogical fingerprint of the granitoid and associated lithologies within the licensed area. Across the dataset, the dominant mineral assemblages are composed of Quartz, Alkali Feldspars (Orthoclase, Microcline, Sanidine), Plagioclase Feldspars (Albite, Anorthite), and Micas (Muscovite, Phlogopite**)**. These mineral modes classify the majority of the samples as Granites, Monzogranites, Syenogranites, and related felsic intrusives, with some samples showing strong evidence of hydrothermal alteration (e.g., Muscovite-rich Greisen).

Key Observations

i. **High Silica Content:** Most samples contain 40–70% Quartz, with some exceeding 60% (classified as Quartzolite or Quartz-rich Granites). This reflects highly evolved, silica-rich magmatism typical of tin-bearing provinces.

ii. **Peraluminous Nature:** Many samples contain appreciable Muscovite (up to 44%), indicating peraluminous compositions. This mineralogical signature is strongly linked to **S-**type granites and greisenization, both of which are classic hosts for cassiterite mineralization.

iii. **Hydrothermal Alteration Indicators:** Several samples (e.g., Muscovite Granodiorites and Muscovite Greisen) show replacement of feldspars by quartz and muscovite. Such alteration is diagnostic of late-stage, fluid-rich magmatic systems where cassiterite is typically precipitated.

iv. **Absence of Cassiterite Peaks:** Cassiterite (SnO_2) was not detected by XRD in the analyzed samples. This is not unexpected, as cassiterite often occurs in low modal abundance, disseminated grains, or veinlets below the detection limit of bulk XRD (usually ~1–2%).

v. **Petrogenetic Implication:** The classification of several samples as Syenogranites, Muscovite-rich Monzogranites, and Greisenized rocks places them squarely within the tin granite lineage, confirming that the intrusive suite is genetically prospective for cassiterite mineralization.

Significance to Cassiterite Exploration

- **Favorable Host Rocks:** The predominance of felsic, silica-rich, and peraluminous granitoids provides a strong geological basis for cassiterite exploration. These rocks are globally recognized as the principal hosts of primary tin deposits.

- **Hydrothermal Processes:** The greisenized samples highlight active fluid–rock interaction, which is the critical process responsible for mobilizing and concentrating tin.

- **Targeting Strategy:** Although cassiterite itself was not identified in the bulk XRD scans, the mineralogical evidence indicates that the system has undergone the right degree of fractionation and alteration to form tin deposits. Exploration efforts should therefore prioritize structurally controlled greisen zones, quartz-rich veins, and muscovite-altered granites that have been identified through mapping and trenching.
- **Integration with Geochemistry:** The absence of cassiterite in XRD is balanced by geochemical assays, where Sn anomalies, even if subtle, can confirm mineralization in these evolved granites.

In summary, the XRD results confirm that the licensed area is underlain by highly evolved, peraluminous granites with evidence of greisenization. These lithologies are strongly associated with cassiterite mineralization worldwide. While cassiterite itself was not detected by XRD (likely due to its low abundance or fine grain size), the host rock composition and alteration signatures provide a positive exploration signal, justifying follow-up targeting.

3.3 Interpretation of Rock Sample Geochemistry - XRF

The analysis of rock samples collected during the geological mapping phase revealed several occurrences of cassiterite mineralization in the bedrock. A total of 47 rock samples (Figure 2) were collected and analyzed. Using a 0.30% SnO_2 cutoff reveals robust tin-bearing mineralization within the license, as 26 of 44 rock samples (59.1%) exceed the threshold, with SnO_2 concentrations ranging from 0.01% to 0.96% (median 0.30%, mean 0.339%). The highest SnO_2 is 0.96% at DMW-614 (rock_id ESR-031); other high-grade rocks include 0.85% at DMW-599 (GR-016), 0.58% at DMW-611 (BGR-028), 0.57% at DMW-593 (GR-010), 0.49% at DMW-609 (BK-026), and 0.48–0.46% at DMW-598 (GR-015), DMW-608 (TL-025), and DMW-594 (GR-011). Grouping anomalous rocks (≥0.30% SnO_2) by code prefix from the rock_id field highlights the principal mineralized areas: GR (7 anomalous samples; median SnO_2 0.46%, max 0.85%), ESR (5; median 0.32%, max 0.96%), BGR (3; median 0.31%, max 0.58%), TL (3; median 0.32%, max 0.46%), LM (3; median 0.34%, max 0.36%), WK (2; median 0.34%, max 0.37%), MJ (2; median 0.335%, max 0.35%), and BK (1; 0.49%). By rock type anomalous counts and grades are: Syenogranite (3 anomalies; median 0.42%, max 0.96%), Granodiorite (3; median 0.49%, max 0.57%), Quartzolite (3; median 0.31%, max 0.46%), Monzogranite (4; median 0.335%, max 0.36%), and single high-grade occurrences in Muscovite Greisen (0.85%), Muscovite Granodiorite (Quartz-rich) (0.58%), and Tonalite (0.37%). Chemically, within this rock dataset, the anomalous class shows lower Fe_2O_3 (median 5.75% vs 6.55% in sub-cutoff rocks), similar P_2O_5 (both 0.06%), higher ZrO_2 (median 0.17% vs 0.11%), and slightly higher Nb_2O_5 (median 0.025% vs 0.020%); Ta_2O_5 medians are the same at 0.04%. Rank correlations across the rocks indicate SnO_2 is negatively associated with Fe_2O_3 and P_2O_5, and weakly positive with Ta_2O_5 and ZrO_2, while Nb_2O_5 and TiO_2 show negligible overall monotonic ties. Taken together, these results delineate Gurungu and Estoyaki areas as the most prominent tin-bearing clusters (by count and/or grade), with additional significant mineralization indicated at Bangotama, Tulu, Lemoro, Wulkai, Maje Uku, and Ba Karpa. The chemistry further shows that tin enrichment in rocks here is not coupled to iron, and that zircon (ZrO_2) and tantalum oxides (Ta_2O_5) are the most consistent accessory indicators alongside cassiterite in the anomalous set.

This pattern of dispersed, low- to medium-grade tin in the source rock is a classic characteristic of this geological province. The anomalous rock samples serve as a compelling indicator of the primary tin source that, over geological time, has weathered to produce the secondary placer and residual deposits. The widespread nature of these anomalies suggests that the source of the cassiterite is robust and not confined to a single, small lode, thus providing a strong foundation for the formation of a significant secondary resource.

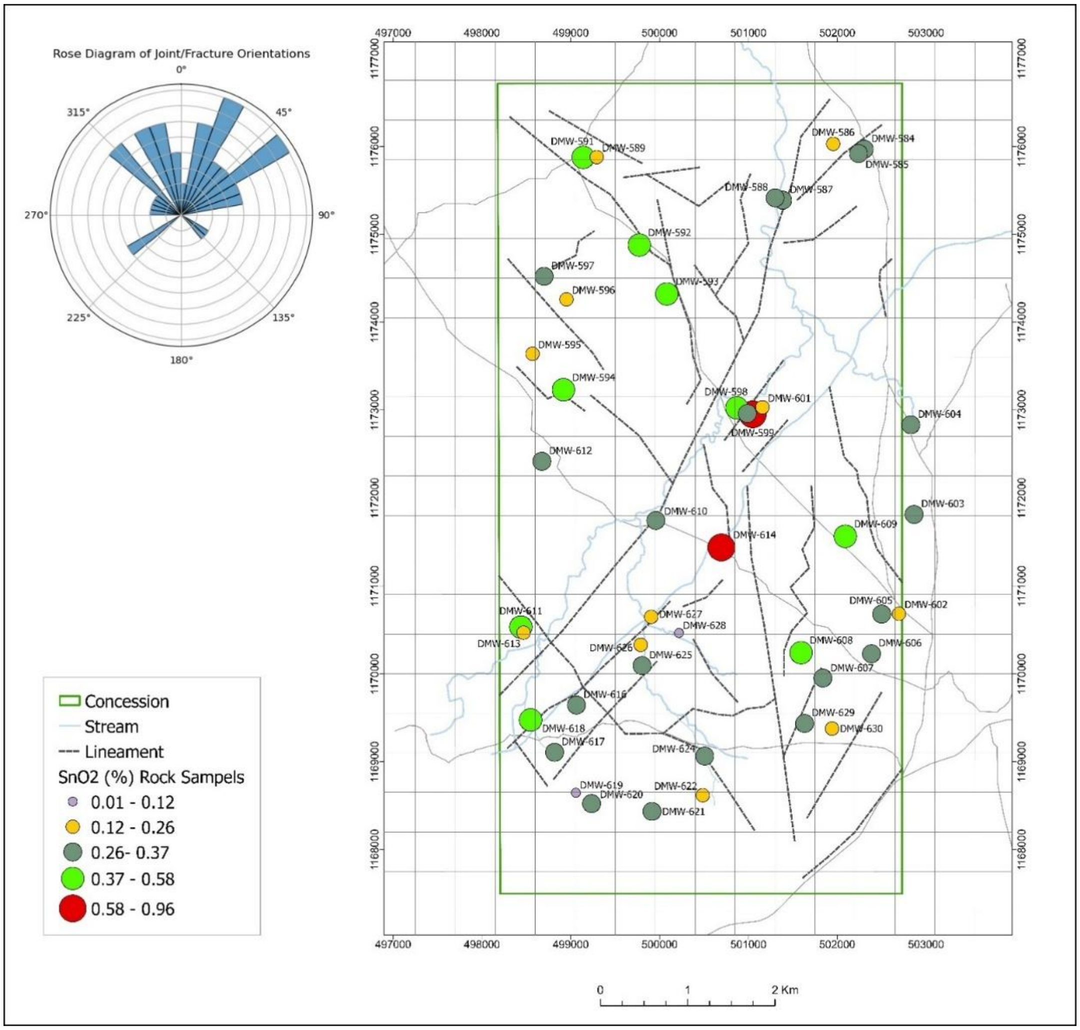

Figure 2 Concentration of Tin Oxide in Rock Samples

Statistical Correlation

Group 1 (> 63% SiO_2)

The correlation analysis (Figure 3) of the high-silica series revealed a distinct geochemical signature surrounding SnO_2 mineralization. The strongest positive correlations were observed with K_2O (0.30), Ag_2O (0.25), Rb_2O (0.19), Al_2O_3 (0.12), and SO_3 (0.10). These relationships suggest that cassiterite mineralization is geochemically linked with potassic alteration, silver enrichment, and granitic fractionation processes, which are typical in highly evolved granite systems. Conversely, strong negative correlations were identified with NiO (-0.47), WO_3 (-0.45), TiO_2 (-0.34), Cs_2O (-

0.25), and MnO (-0.23). These minerals represent depleted phases in Sn-rich environments, particularly highlighting the reduced presence of mafic and tungsten-bearing minerals, which is consistent with the fractionation-driven evolution of Younger Granites, where tin and tungsten mineralization occur in separate domains.

The scatter plots (Figure 4) between SnO_2 and these associated minerals further confirmed these trends. Samples with elevated SnO_2 values consistently showed enrichment in K_2O, Ag_2O, and Rb_2O, reinforcing their value as pathfinders in cassiterite exploration. In contrast, high SnO_2 concentrations coincided with depletion in NiO, WO_3, and TiO_2, producing a clear geochemical contrast between cassiterite-bearing and non-mineralized zones. These scatter patterns provide practical exploration vectors, where zones of simultaneous enrichment and depletion can be mapped and targeted.

Principal component analysis (Figure 5) provided a multidimensional view of these relationships. The PCA biplot showed that SnO_2 clusters closely with K_2O, Ag_2O, Rb_2O, Al_2O_3, and SO_3, emphasizing their strong association with tin mineralization. On the opposite side of the biplot, NiO, WO_3, TiO_2, Cs_2O, and MnO vectors pointed away from SnO_2, reinforcing their role as depletion indicators. The first two principal components explained virtually all the variance in the data, confirming that the selected minerals provide a highly representative framework for distinguishing cassiterite mineralization geochemically.

Taken together, the correlation heatmap, scatter plots, and PCA analysis establish a robust geochemical fingerprint for cassiterite mineralization within the studied area. SnO_2 enrichment is closely linked to potassic and silver-bearing phases, with rubidium and alumina providing additional supportive signals, while nickel, tungsten, titanium, cesium, and manganese are characteristically depleted. This dual fingerprint of enrichment and depletion creates a strong exploration tool, guiding geologists toward zones of cassiterite mineralization with higher accuracy by focusing on areas where potassic and silver enrichment coincide with the absence of mafic and tungsten phases.

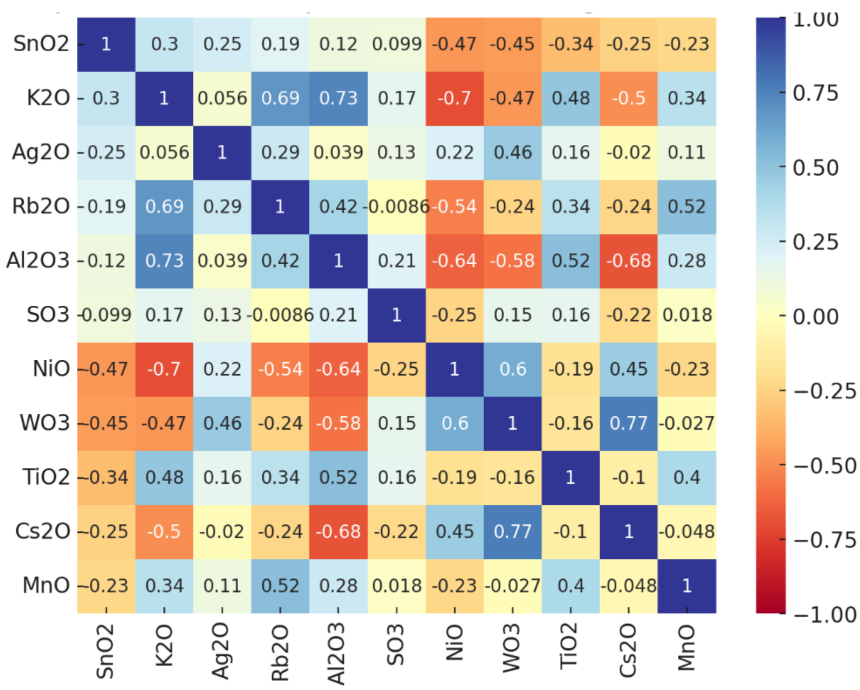

Figure 3 Correlation Heatmap of Granitic rocks with >63% Silica oxide

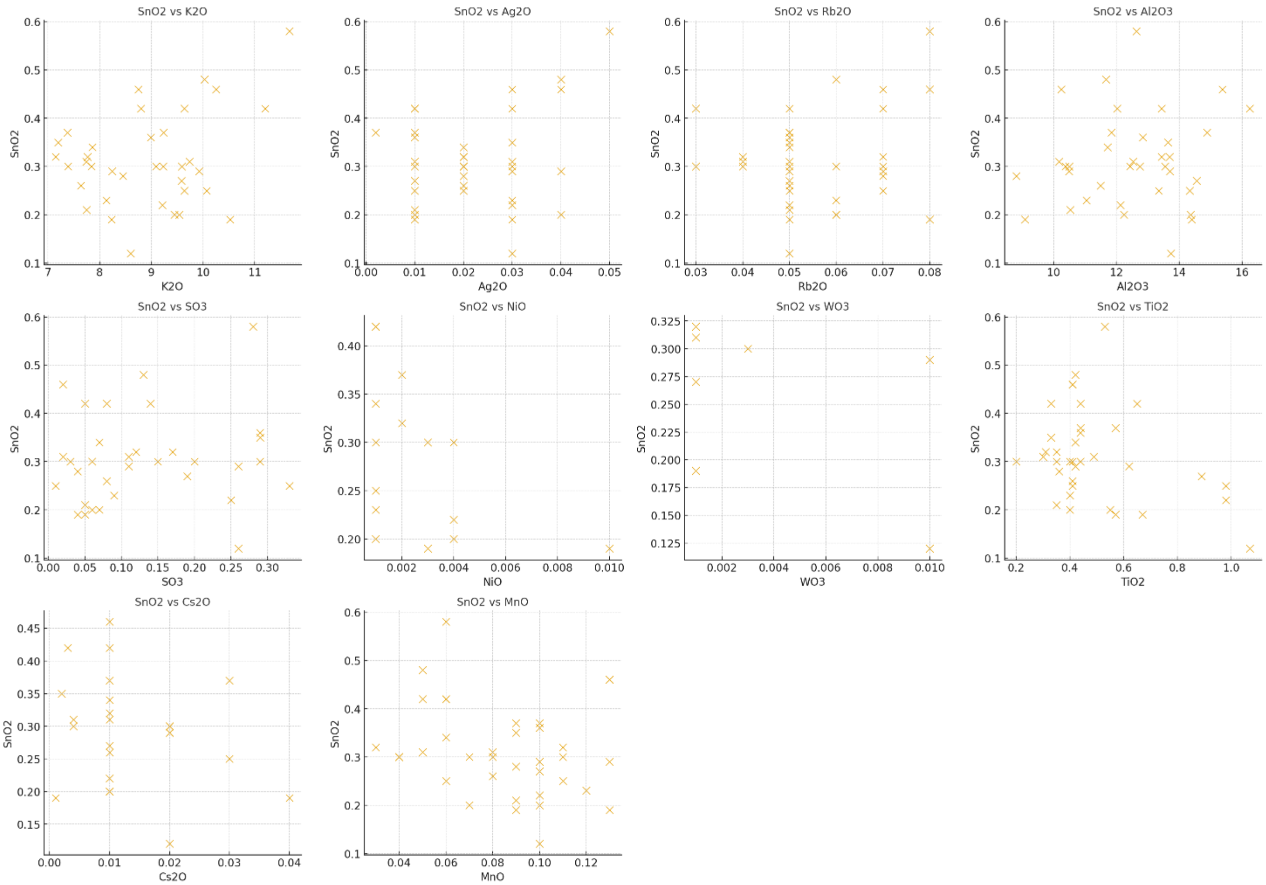

Figure 4 Scatter plots of Group 1 phase with >63% Silica oxide

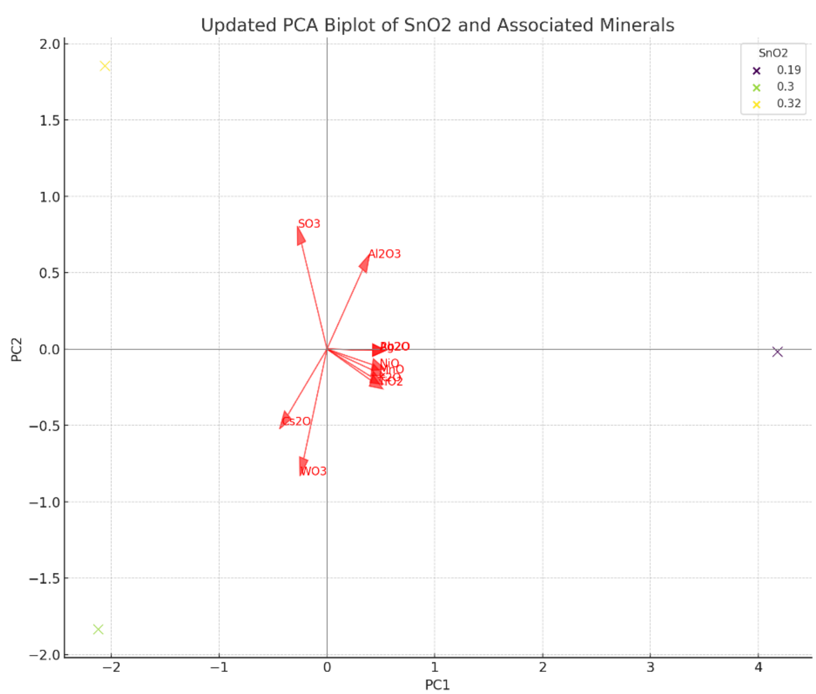

Figure 5 PCA Plot of Sn02 and Associated Minerals in the Group 1 phase

Group 2 (53-56 % SiO_2)

The correlation analysis of the intermediate silica oxide group reveals an evident geochemical fingerprint for cassiterite mineralization. SnO_2 shows the strongest positive relationship with WO_3 (0.93), followed by K_2O (0.84), SiO_2 (0.77), NiO (0.75), and BaO (0.56). This strong association between SnO_2 and WO_3 is highly significant, as it suggests that tin mineralization within this dataset is closely linked with tungsten-bearing phases, pointing to a Sn–W system that is common in highly evolved granitic environments. The enrichment in K_2O further indicates potassic alteration, which is typical of late-stage granite fractionation processes that often concentrate tin. The positive correlation with silica (SiO_2) reflects the quartz-rich character of the mineralizing granites. At the same time, the moderate associations with NiO and BaO may highlight subtle geochemical pathways where nickel and barium remain in trace concentrations in cassiterite-bearing rocks.

On the opposite side, SnO_2 exhibits strong negative correlations with TiO_2 (-0.93), Fe_2O_3 (-0.86), MnO (-0.81), CaO (-0.76), and Cs_2O (-0.61). These trends reflect a distinct depletion of titanium, iron, manganese, and calcium phases in areas enriched with cassiterite. Such depletion patterns align with the behavior of highly evolved granites, where ferromagnesian and calcium-bearing minerals are progressively removed during fractionation, leaving behind residual melts enriched in tin, tungsten, and alkalis. The negative correlation with Cs_2O is also noteworthy, as it indicates a contrasting geochemical environment where cesium is not enriched in the same zones as tin, possibly reflecting differences in mineral partitioning during crystallization. These depletions provide strong discriminant signals that can help vector towards cassiterite-rich zones.

The PCA biplot provides a multidimensional confirmation of these relationships. SnO_2, WO_3, K_2O, and SiO_2 cluster together on the positive axis, underscoring their close geochemical association and reinforcing the interpretation of a Sn–W–K–Si assemblage. By contrast, TiO_2, Fe_2O_3, MnO, and CaO project in the opposite direction, clearly separating the mineralizing environment from mafic and iron-titanium-bearing assemblages. The PCA explains 78.7% of the total variance, which is substantial, meaning that the first two principal components capture the dominant geochemical processes controlling cassiterite mineralization in this dataset.

Taken together, the evidence points to a tin–tungsten association in a strongly fractionated granitic system. The enrichment of WO_3, K_2O, and SiO_2 alongside SnO_2 reflects the geochemical evolution of mineralizing granites where potassic alteration, quartz enrichment, and tungsten mineralization converge. At the same time, the consistent depletion of TiO_2, Fe_2O_3, MnO, and CaO provides a strong negative geochemical fingerprint, marking areas where cassiterite is most likely to occur. This dual signature, positive enrichment in pathfinder elements, and depletion of contrasting mafic and iron-rich phases, provides a robust exploration tool for targeting cassiterite mineralization within the studied area.

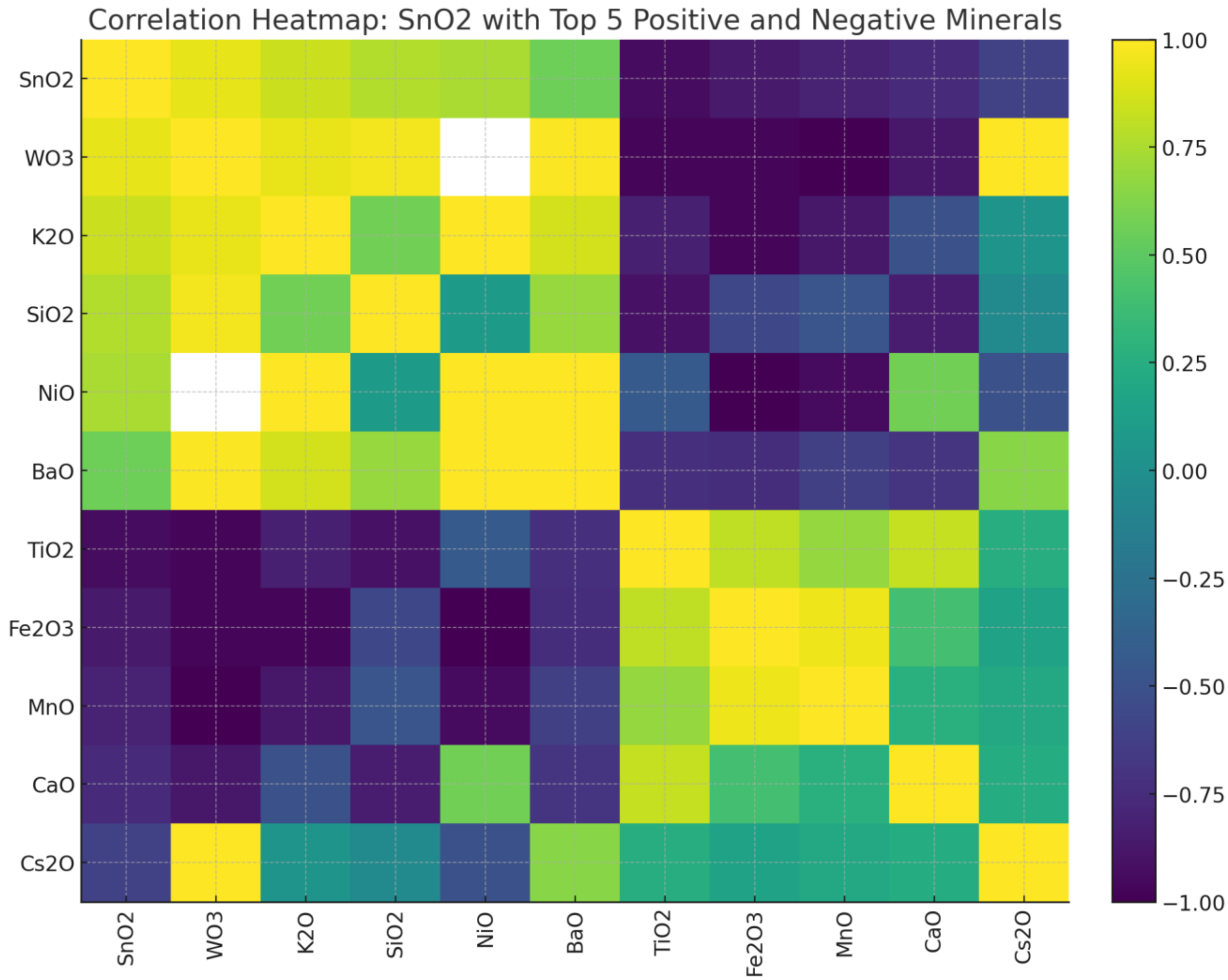
Correlation Heatmap: SnO2 with Top 5 Positive and Negative Minerals
SnO2
WO3
K2O
SiO2
NiO
BaO
TiO2
Fe2O3
MnO
CaO
Cs2O
1.00
0.75
0.50
0.25
0.00
−0.25
−0.50
−0.75
−1.00

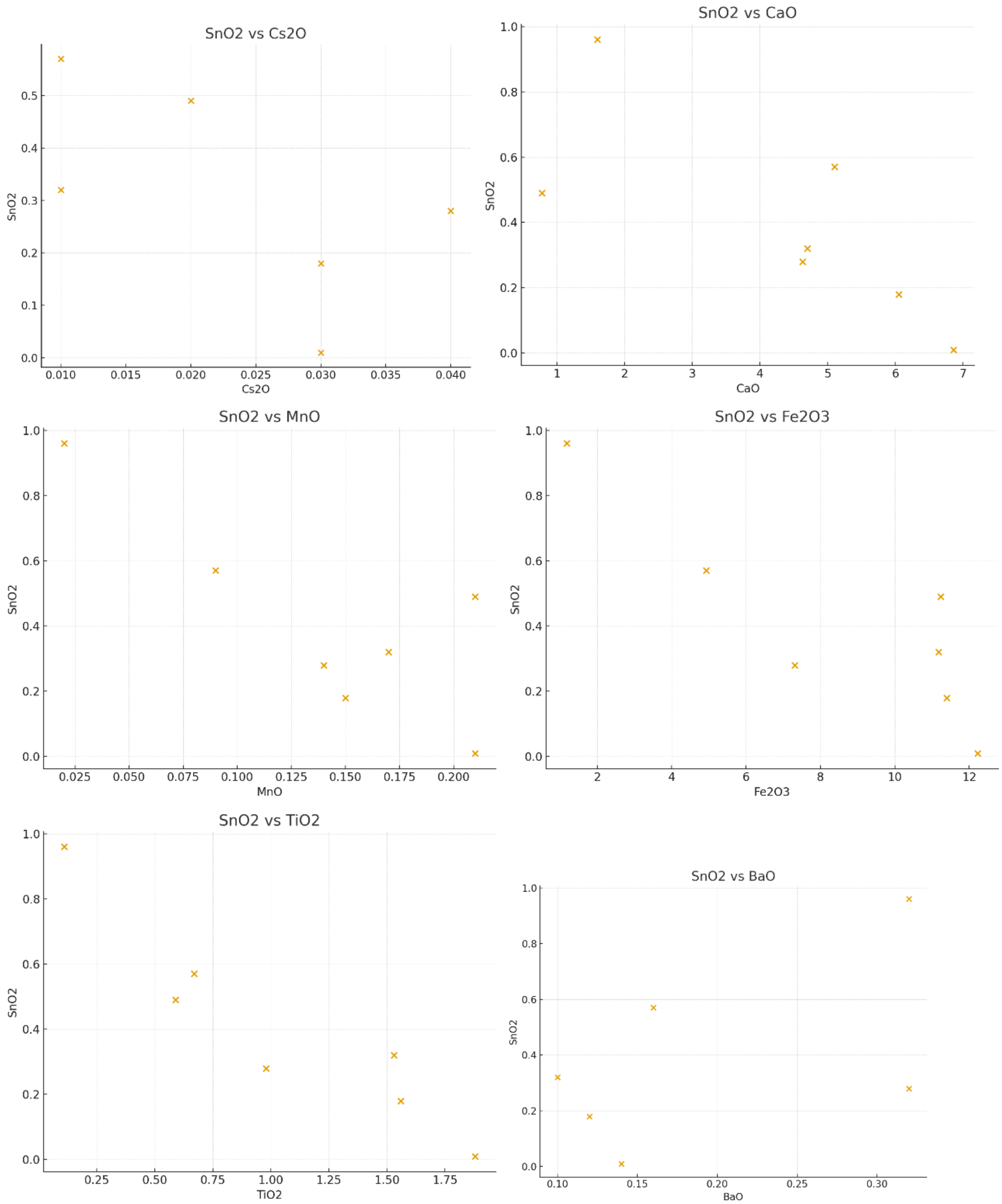

Figure 6 Scatter plots of Group 2 phase with 53-63% Silica oxide

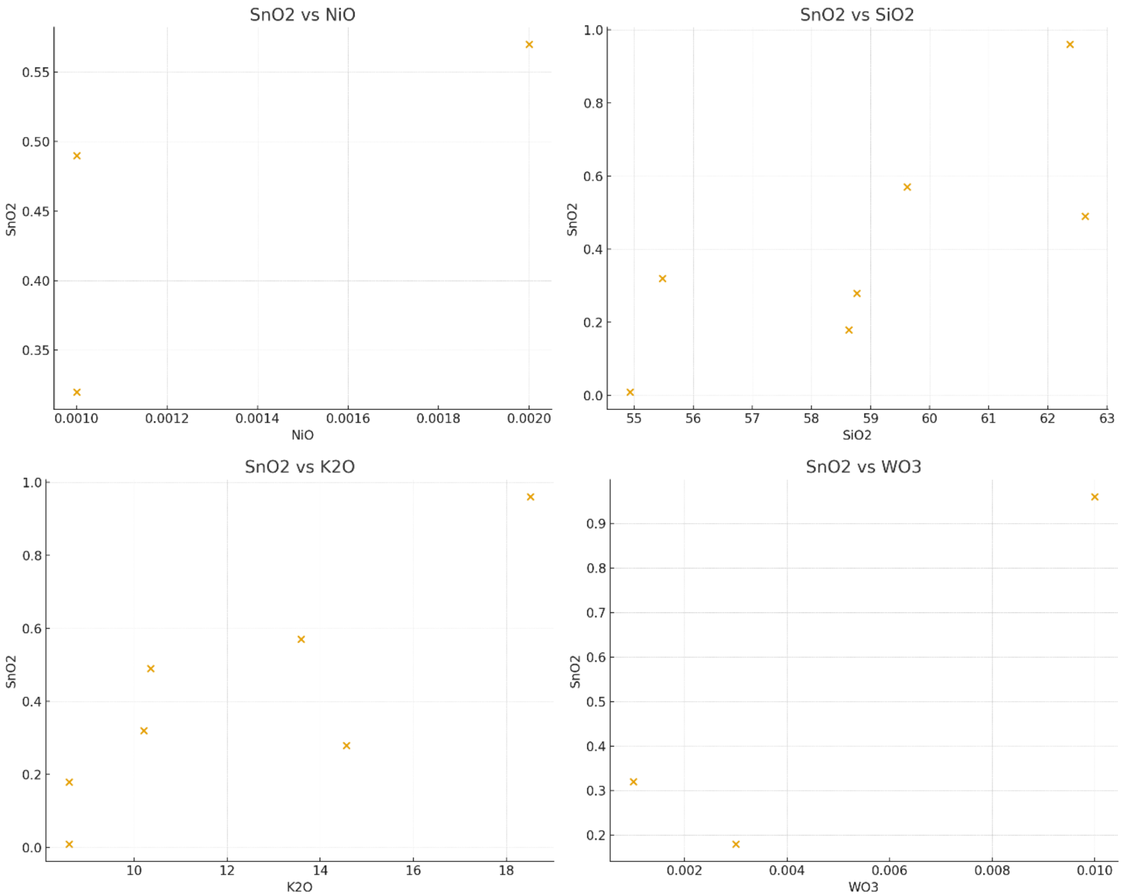

Figure 7 Scatter plots of Group 2 phase with 53-63% Silica oxide

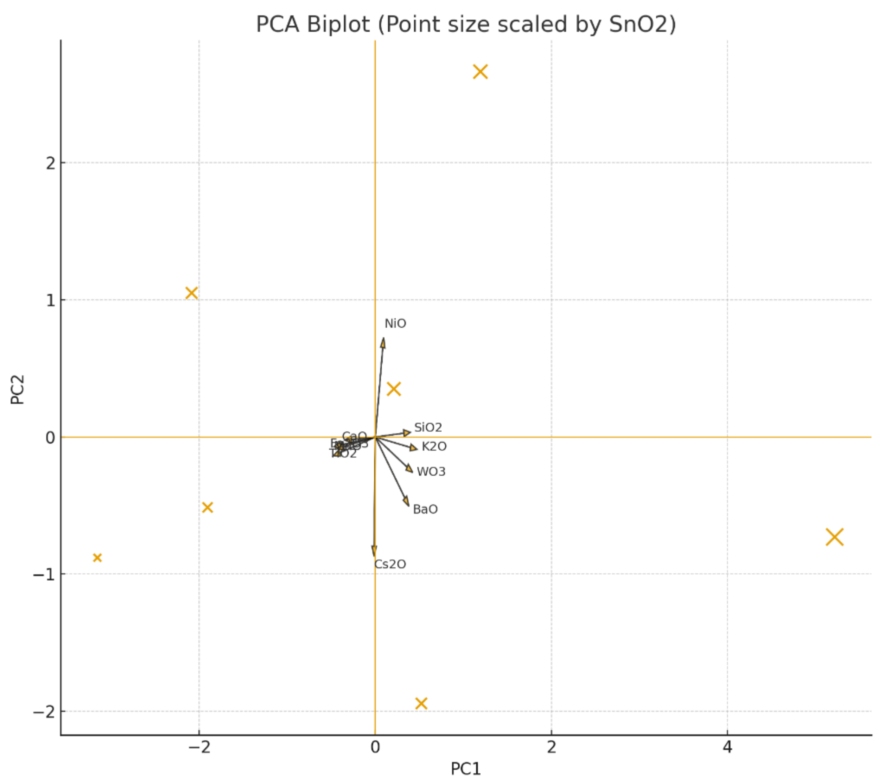

Figure 8 PCA Plot of $Sn0_2$ and Associated Minerals in the Group 2 phase

3.4 Pitting and Soil Samples

Horizon A

The geochemical results from the soil samples in the licensed area, all classified within Interval A, reveal a total of 162 analyses, of which 14 samples (8.64%) exceeded the 0.2% SnO_2 cutoff used as the threshold for cassiterite occurrence. SnO_2 concentrations range from below detection to a maximum of 0.85% in pit ES-033 (sample DMW-353), with additional notable anomalies including EST-012 (0.55%), EST-063 and EST-068 (0.52% each), BGS-023 (0.48%), and BGS-025 (0.43%). These anomalies establish discrete priority pits for follow-up exploration. The median SnO_2 level is 0.08%, indicating that most samples fall below background levels; however, the anomalous cluster defines a distinct subset of high-grade samples. When compared to background soils (<0.2% SnO_2), anomalous samples exhibit slightly higher P_2O_5 (0.12% vs 0.08%), indicating an association with phosphate minerals such as monazite, which is an important index mineral in cassiterite-bearing systems of the Younger Granites. Correlation analysis further reveals that SnO_2 exhibits weak positive associations with Ta_2O_5 and ZrO_2, indicating a shared geochemical environment with tantalum and zircon, both of which are commonly associated with granitic rare-metal mineralization. By contrast, Fe_2O_3 shows a weak negative correlation with SnO_2, and median values of iron and titanium oxides are slightly lower in anomalous samples, indicating that elevated iron does not consistently track cassiterite anomalies in this dataset. The chemical signature of the highest-grade sample (0.85% SnO_2) illustrates this pattern, combining very high tin oxide with moderate P_2O_5 (0.14%) and relatively subdued Fe_2O_3 (5.16%). Taken together, the dataset defines a small but significant proportion of anomalous pits in Interval A soils, characterized by SnO_2 enrichment with coincident phosphate and rare-metal indicators, which should be prioritized for deeper interval sampling (B–D), trenching, and confirmatory mineralogical analysis.

For Interval A, the correlation plot (Figure 9) displays a distinct pattern. SnO_2 exhibits a weak negative correlation with Fe_2O_3 (–0.23), suggesting that higher tin values are not associated with iron enrichment. Similarly, SnO_2 vs P_2O_5 shows a weak negative trend (–0.14), although the anomalous samples had slightly higher median P_2O_5 values, suggesting an occasional linkage to phosphate minerals, such as monazite. The most notable positive associations are with Ta_2O_5 (+0.21) and ZrO_2 (+0.15), both of which are reliable index minerals in Younger Granite terrains, marking the presence of cassiterite-bearing systems. Nb_2O_5 shows almost no correlation (–0.01), while TiO_2 is essentially neutral. Overall, the Interval A plot suggests that tantalum and zircon are the most consistent geochemical companions to cassiterite anomalies, whereas iron and phosphate enrichment are not reliable indicators in this horizon.

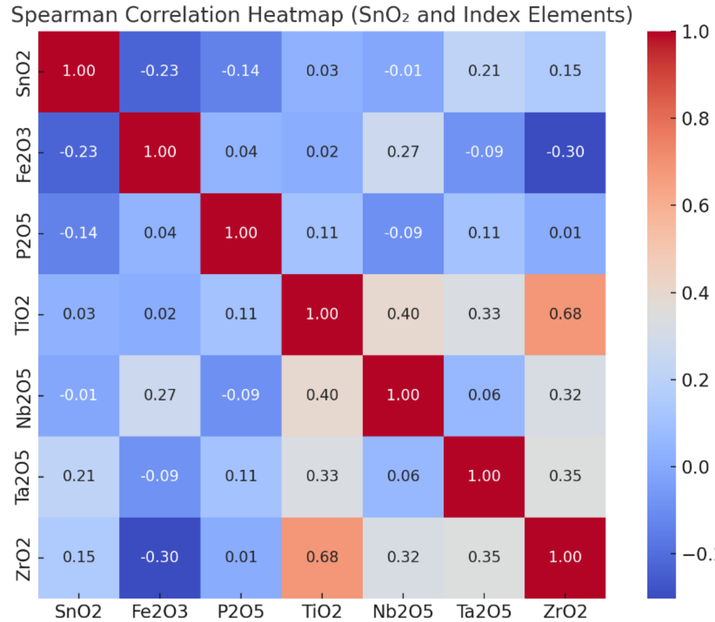

Figure 9 Correlation Heatmap of Tin Oxide and other elements for Horizon A

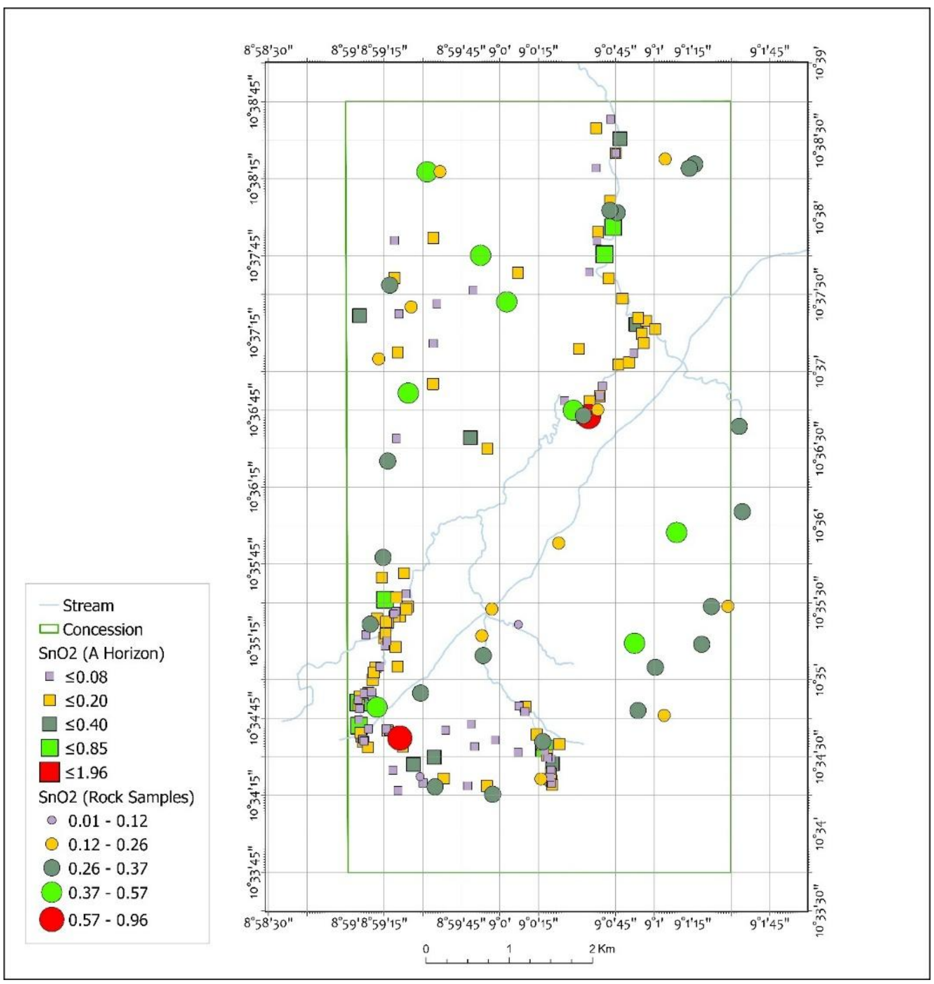

Figure 10 Concentration of Tin Oxide in the Soil sample (Horizon A) superimposed on Rock Samples.

Horizon B

A total of 162 soil samples were analyzed for Interval B. Tin oxide (SnO_2) concentrations range from 0.00 to 1.96%, with a median of 0.03% and a mean of 0.078%. Applying the 0.2% SnO_2 cutoff for cassiterite mineralization, 15 samples (9.26%) qualify as anomalous. The most significant anomaly is at pit EST-053, which returns 1.96% SnO_2, an exceptionally high value for soil geochemistry and strongly indicative of cassiterite enrichment. Other notable anomalous pits include EST-072 (0.33%), EST-079 (0.38%), BGS-029 (0.33%), and EST-015 (0.31%). These pits form the core targets for follow-up evaluation.

Associations with Index Elements

Correlation analysis provides insights into mineralogical associations relevant to the Younger Granite cassiterite system:

- **SnO_2 vs Fe_2O_3:** A strong negative correlation (–0.54) indicates that cassiterite enrichment is not coupled with iron oxide abundance. This suggests that the anomalous tin is concentrated independently of lateritic or ferruginous enrichment processes.

- **SnO_2 vs P_2O_5:** Weak negative association (–0.19). Unlike Interval A (where SnO_2 and P_2O_5 occasionally rose together), here, cassiterite anomalies are not consistently accompanied by phosphate enrichment. This limits the use of P_2O_5 as a monazite proxy in Interval B soils.

- **SnO_2 vs Ta_2O_5 and ZrO_2:** Moderate positive correlations with Ta_2O_5 (+0.29) and ZrO_2 (+0.47) highlight an association between tin anomalies and heavy mineral phases such as tantalite–columbite and zircon. These are classic index minerals in rare-metal granite terrains, reinforcing the genetic link between cassiterite and granitic accessory minerals.

- **SnO_2 vs TiO_2 and Nb_2O_5:** Weak positive associations (+0.15 and +0.12, respectively) suggest that titanium and niobium oxides occur sporadically alongside cassiterite but are not robust pathfinders in this interval.

The geochemical results from Interval B indicate that nearly one in ten samples exceeds the cassiterite cutoff, confirming that cassiterite mineralization is not restricted to surface soils (Interval A) but extends to depth. The extremely high SnO_2 content at EST-053 (1.96%) demonstrates continuity of tin enrichment into the B horizon, strengthening the case for deep residual deposits within the license area. The positive associations with Ta_2O_5 and ZrO_2 validate the exploration model for Younger Granites, where cassiterite commonly co-occurs with rare-metal oxides and resistant heavy minerals. Conversely, the negative correlation with Fe_2O_3 indicates that ferruginization should not be relied upon as a geochemical guide for tin.

In conclusion, Interval B soils exhibit significant cassiterite mineralization, as indicated by multiple anomalies exceeding the 0.2% cutoff and one extreme value of approximately 2% SnO_2. These results justify systematic follow-up, including detailed pit logging, trenching, and targeted sampling of heavy mineral concentrates to trace the tin-bearing zones and their association with tantalum and zirconium phases.

The correlation plot for Interval B highlights the geochemical relationships among SnO_2 and key index elements. The most significant feature is the strong negative correlation between SnO_2 and Fe_2O_3 (–0.54), indicating that tin enrichment does not coincide with iron oxide accumulation and that ferruginization is not a reliable indicator of cassiterite presence in this horizon. In contrast, SnO_2 shows moderate positive correlations with Ta_2O_5 (+0.29) and ZrO_2 (+0.47), reflecting the shared association of cassiterite with tantalum–niobium oxides and zircon, both typical accessory minerals in rare-metal granites. The weak positive correlation with TiO_2 (+0.15) and Nb_2O_5 (+0.12) suggests occasional but inconsistent co-occurrence with titanium and niobium phases. Overall, the plot confirms that cassiterite anomalies in Interval B are best tracked through heavy mineral pathfinders, such as tantalum and zircon, while iron enrichment is inversely related.

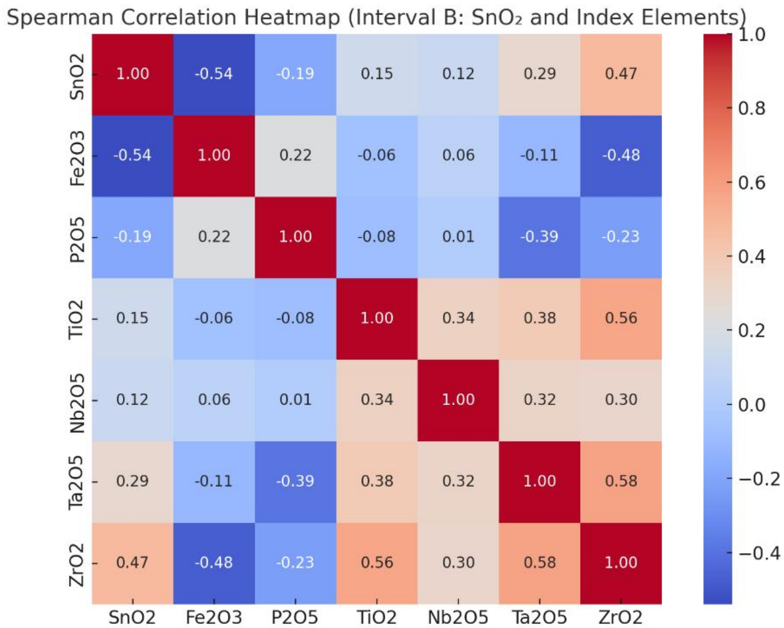

Figure 11 Correlation Heatmap of Tin Oxide and other elements for Horizon B

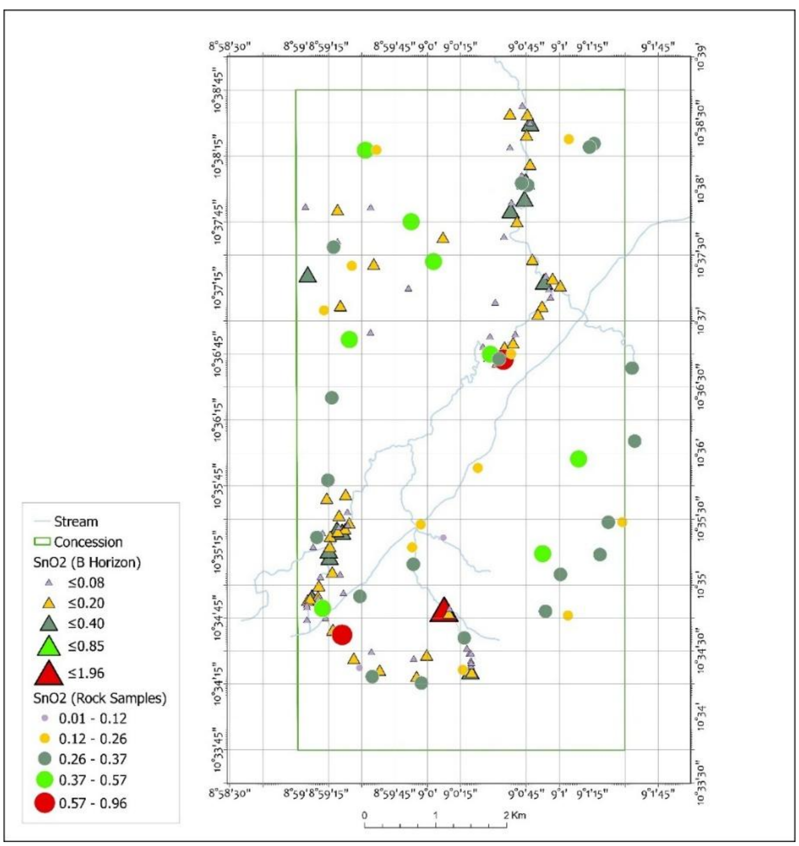

Figure 12 Concentration of Tin Oxide in the Soil sample (Horizon B) superimposed on Rock Samples.

Horizon C

Interval C contains 150 soil analyses. SnO_2 ranges 0.00–0.51%, with median 0.02% and mean 0.067%. Applying the 0.2% threshold identifies 13 anomalous samples (8.67%). The highest value is 0.51% SnO_2 at pit BGS-021 (sample DMW-533); associated chemistry for this peak sample includes Fe_2O_3 12.25%, TiO_2 2.91%, Ta_2O_5 0.04%, ZrO_2 0.56% (P_2O_5 not reported for that sample). Per-pit tallies show multiple single-sample anomalies distributed across pits rather than a single pit contributing many Interval-C anomalies; those pits form the initial targets for follow-up within this horizon (see the anomaly table provided).

Spearman rank correlations for Interval C show a moderate positive association of SnO_2 with ZrO_2 (+0.51) and a weaker positive association with Ta_2O_5 (+0.27), confirming that tin anomalies tend to occur with zircon and tantalum-bearing phases in this interval—index minerals consistent with rare-metal granite signatures. SnO_2 vs TiO_2 is weakly positive (+0.20), indicating some co-occurrence with titanium-rich heavy minerals. In contrast, SnO_2 vs Fe_2O_3 is moderately negative (–0.57), showing that higher tin is not coupled with iron oxide enrichment in Interval C soils; ferruginization is therefore not a reliable guide to cassiterite here. SnO_2 vs P_2O_5 is also negative (–0.30) at the dataset level, suggesting that monazite (P_2O_5 proxy) is not consistently elevated within the tin anomalies in this interval.

The presence of 13 Interval-C anomalies ≥0.2% SnO_2, including a maximum of 0.51%, demonstrates that cassiterite enrichment persists into the C horizon rather than being restricted to shallow soils. The positive links with ZrO_2 and Ta_2O_5 underline the value of tracking zircon and tantalum-niobium oxide grains in heavy-mineral separates when following up Interval-C anomalies. Conversely, the negative relationship with Fe_2O_3 indicates that iron oxide abundance should not be used as a proxy for cassiterite in this horizon. Where available, targeted mineralogical checks (e.g., grain mounts or heavy-mineral microscopy) on the anomalous C-interval samples should prioritize zircon and tantalum-bearing species to validate these geochemical associations.

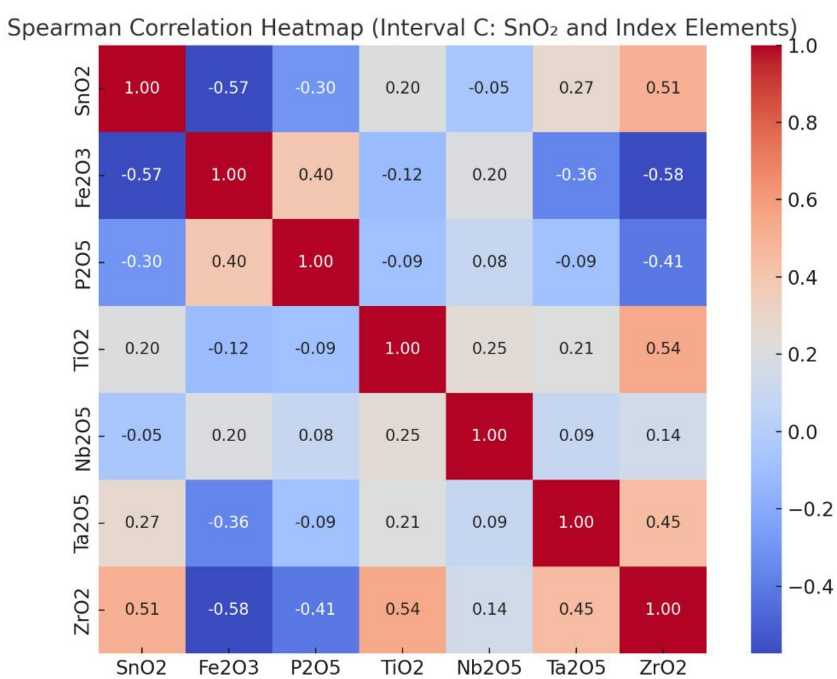

Figure 13 Correlation Heatmap of Tin Oxide and other elements for Horizon C

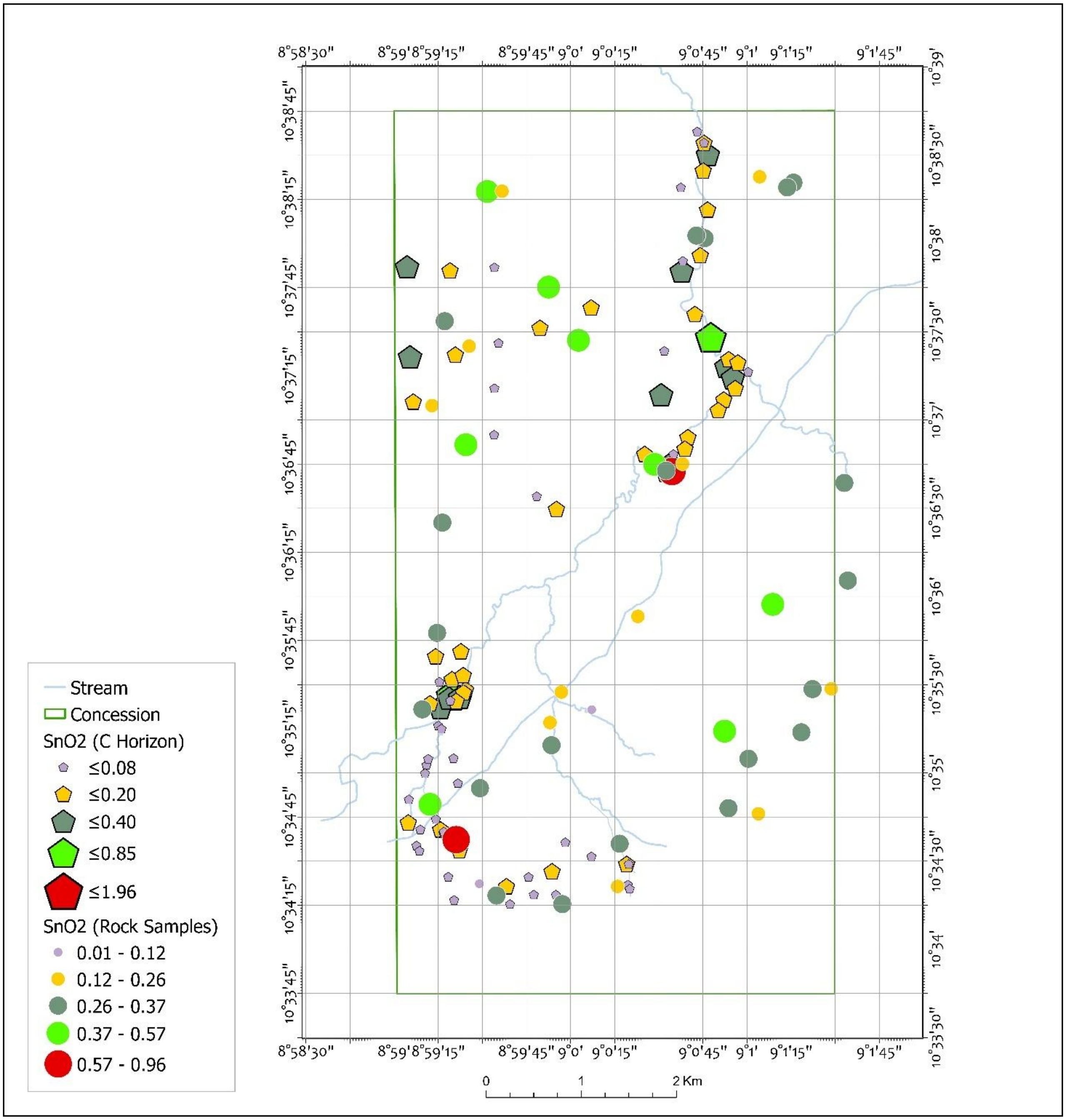

Figure 14 Concentration of Tin Oxide in the Soil sample (Horizon C) superimposed on Rock Samples.

Horizon D

A total of 113 soil samples were analyzed in Interval D. SnO_2 values range from 0.00 to 0.74%, with a median of 0.00% and a mean of 0.068%. Using the 0.2% SnO_2 cutoff, 12 samples (10.6%) are classified as anomalous, marking this interval as the most anomalous proportionally compared to A–C. The standout anomaly is at pit EST-058, with 0.74% SnO_2, while other notable values include 0.40% (BG-027), 0.34% (BGS-017), 0.28% (BGS-029 and EST-080), and 0.27% (EST-085). These anomalies confirm the persistence of cassiterite mineralization at deeper soil horizons.

Correlation analysis reveals clear mineralogical associations:

- **SnO_2 vs Fe_2O_3:** A strong negative correlation (–0.56) indicates that high tin grades consistently occur where iron oxide is depleted. This shows that ferruginous enrichment is not a reliable guide for cassiterite in Interval D.

- **SnO_2 vs ZrO_2:** A moderate positive correlation (+0.43) highlights the close association of cassiterite with zircon. This is consistent with resistant heavy mineral assemblages in the Younger Granites.

- **SnO_2 vs Ta_2O_5:** Positive correlation (+0.24), showing that tantalum-bearing phases frequently accompany cassiterite anomalies at depth.

- **SnO_2 vs P_2O_5:** Negative correlation (–0.26), indicating that phosphate (and by extension monazite) enrichment is not consistently coupled with tin in this horizon.

- **SnO_2 vs TiO_2 and Nb_2O_5:** Both show weak positive trends (+0.04 and +0.06), suggesting occasional co-occurrence with titanium and niobium oxides but not strong pathfinder behavior.

Interval D demonstrates that cassiterite mineralization persists and even strengthens in anomaly frequency at depth, with over 10% of samples above the cutoff. The highest SnO_2 value (0.74%) and multiple discrete anomalies confirm the presence of deep residual or eluvial tin enrichment. The positive links with zircon and tantalum reinforce the importance of heavy mineral analysis in anomaly verification. Conversely, the consistent negative association with Fe_2O_3 shows that iron-rich zones should not be mistaken for tin-bearing horizons.

Interval D soils contain a higher proportion of tin anomalies compared to shallower horizons, with SnO_2 enrichment strongly tied to zircon and tantalum oxides but inversely related to iron oxides and phosphate minerals. These findings indicate that cassiterite mineralization extends into deeper weathering horizons and that zircon and tantalum are the most reliable index minerals for follow-up exploration in this interval.

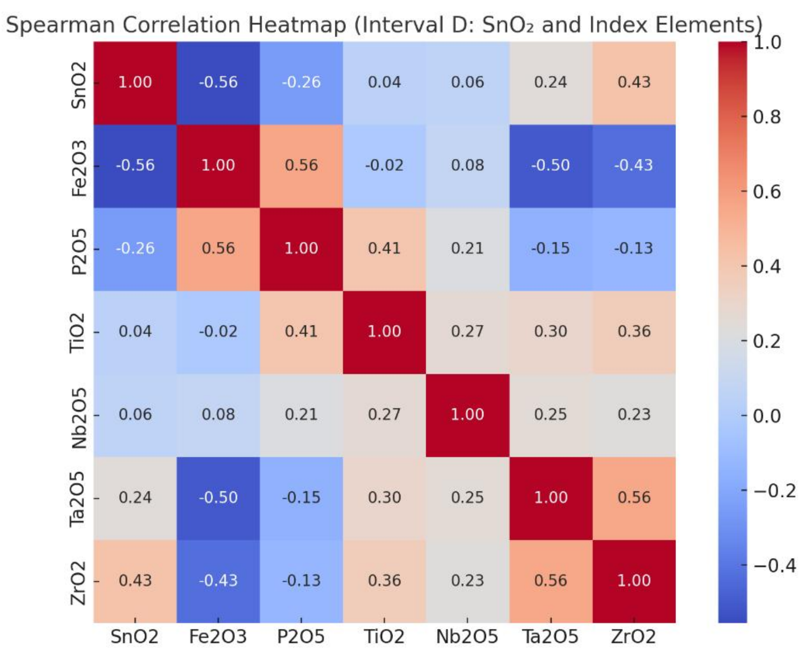

Figure 15 Correlation Heatmap of Tin Oxide and other elements for Horizon D

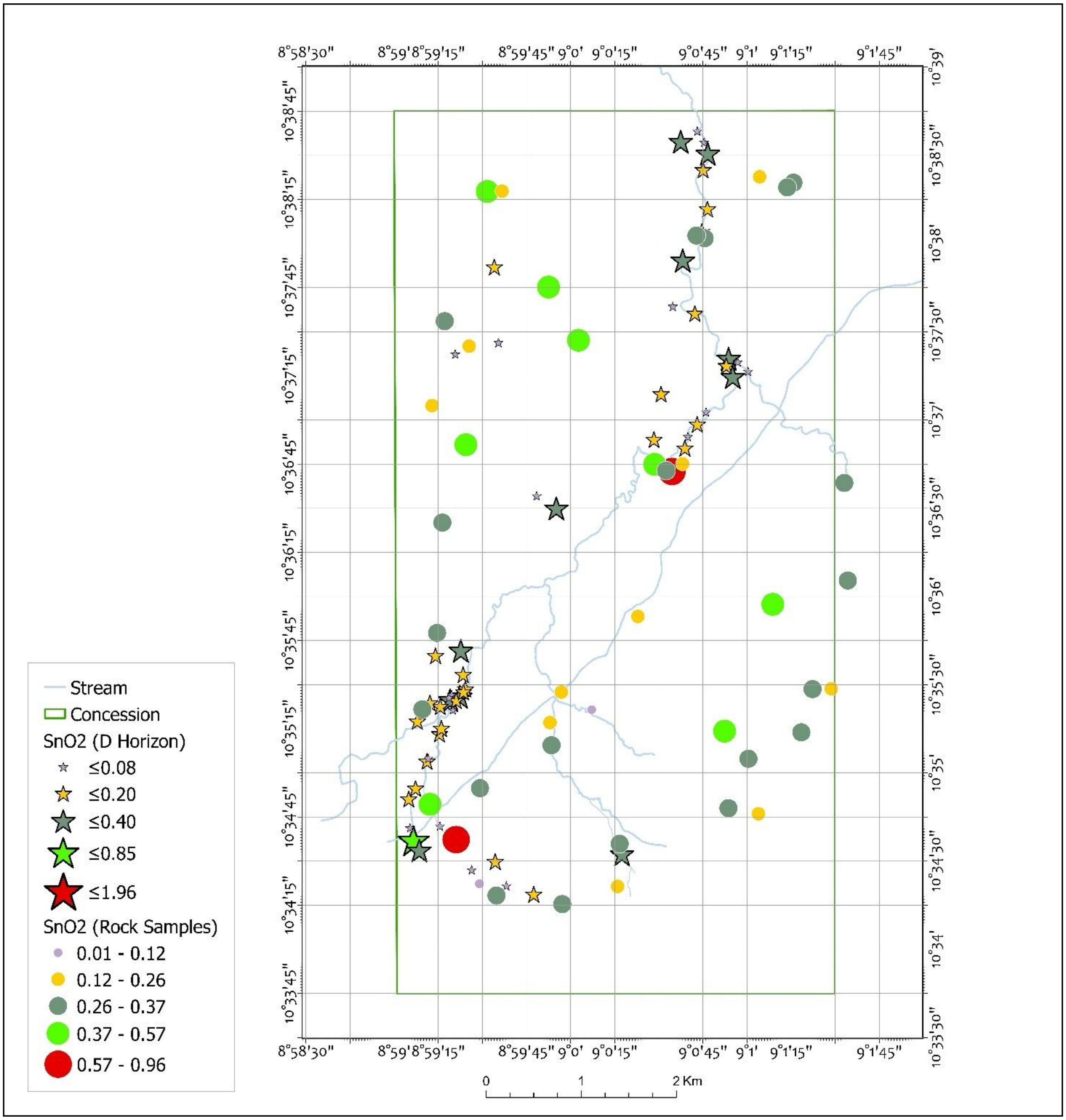

Figure 16 Concentration of Tin Oxide in the Soil sample (Horizon D) superimposed on Rock Samples.

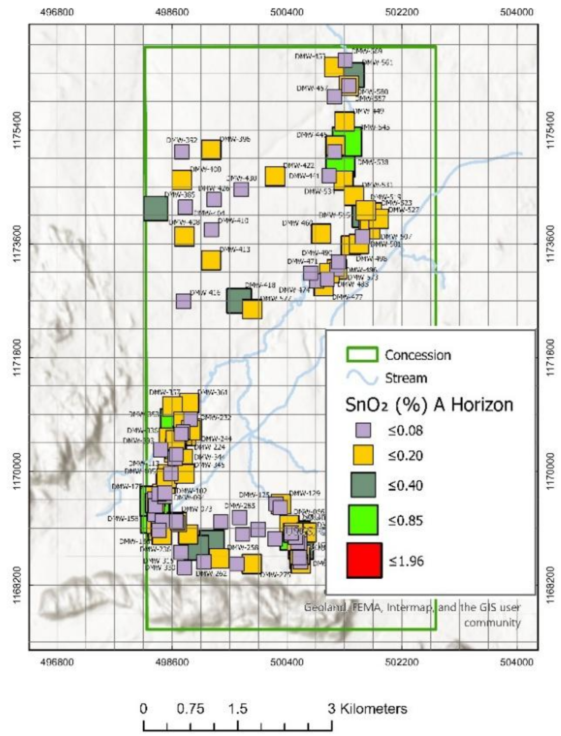

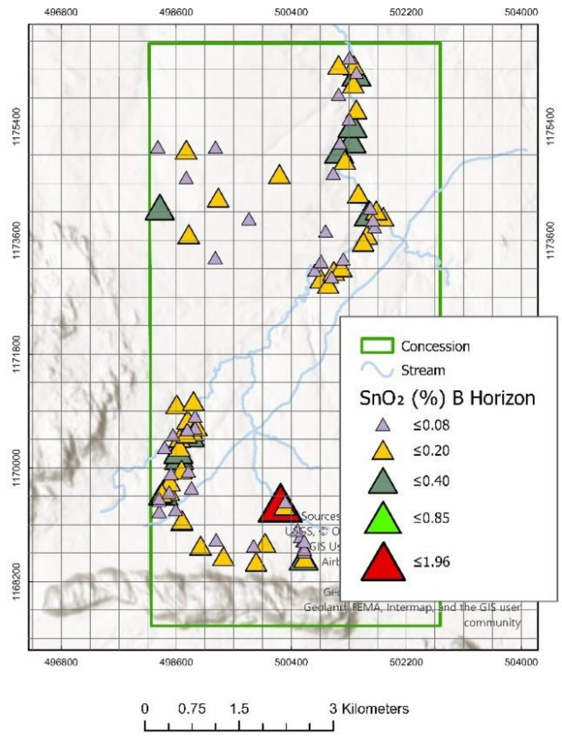

Figure 17 SnO_2 Concentration in Interval A and B

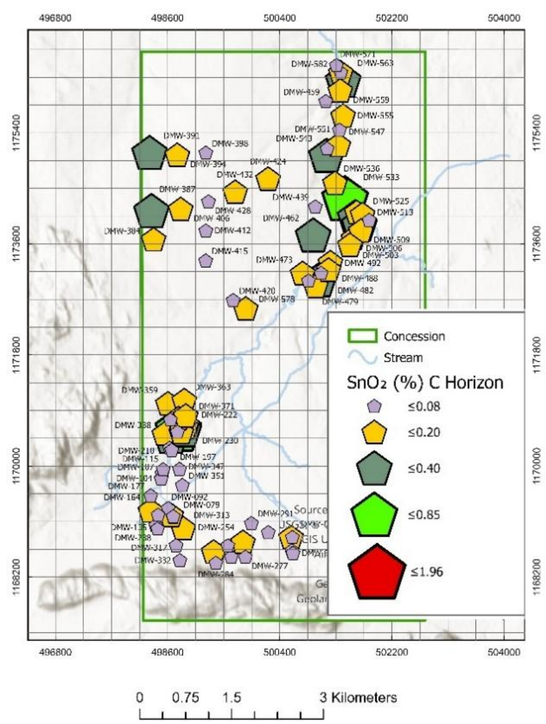

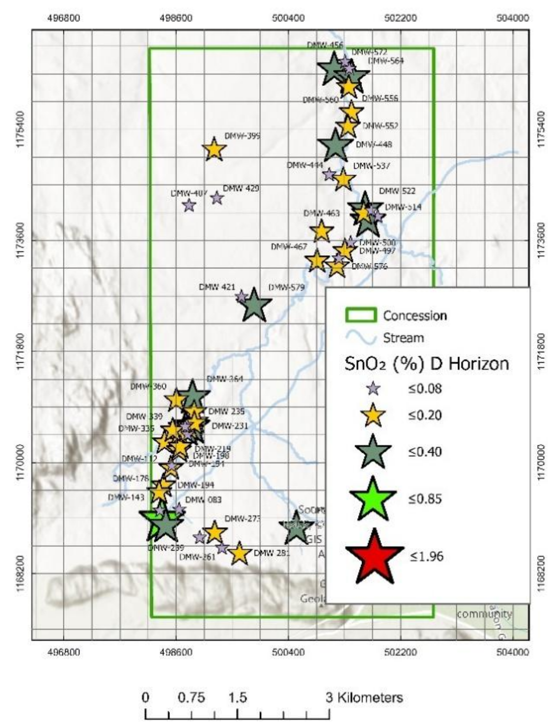

Figure 18 SnO_2 Concentration in interval C and D

The integrated geochemical results from soil Intervals A–D confirm that cassiterite mineralization within the Younger Granite Complex is vertically extensive, with anomalies present from surface to deep horizons. Using a 0.2% SnO_2 cutoff, anomalous samples account for 8.6% in Interval A, 9.3% in Interval B, 8.7% in Interval C, and the highest frequency of 10.6% in Interval D. Grades range from background levels up to 1.96% SnO_2 (Interval B), with additional significant anomalies including 0.85% in Interval A, 0.51% in Interval C, and 0.74% in Interval D, confirming continuity of tin enrichment across the soil profile. Correlation analysis shows that SnO_2 is consistently and positively associated with zircon (ZrO_2) and tantalum oxides (Ta_2O_5), making these the most reliable pathfinders. At the same time, Fe_2O_3 exhibits strong negative correlations and P_2O_5 shows weak to negative associations, indicating that ferruginization and phosphate enrichment are not dependable guides to cassiterite. TiO_2 and Nb_2O_5 display weak positive trends and are of secondary importance. Overall, the geochemical evidence demonstrates a deep residual cassiterite system with zircon and tantalum as key companion minerals, justifying further trenching, bulk sampling, and heavy mineral analysis to delineate ore-bearing zones.

CHAPTER FOUR

4.0 COMPARATIVE ANALYSIS OF CASSITERITE MINERALIZATION

4.1 Comparison to Other Nigerian Tin Deposits

The exploration results from the Tulu project are directly comparable to and consistent with the historical and contemporary tin mining activities in other parts of Nigeria. Tin mineralization in Nigeria is predominantly associated with the Younger Granites, which serve as the primary source rocks for cassiterite.[2] The vast majority of Nigeria's tin has been extracted from alluvial and residual deposits on the Jos Plateau, derived from the weathering of these granitic complexes.[2]

The Tulu project exhibits the same key characteristics: the presence of anomalous tin in granitic rock samples, indicating a primary source, and the accumulation of high-grade cassiterite in the overlying regolith and stream sediments, suggesting a viable secondary, or placer-style, deposit.[9] This congruence with the established geological model provides a high degree of confidence in the project's potential. The Tulu licensed area appears to be a natural extension of the same metallogenic processes that have made the Jos Plateau a historically significant region for tin production.

4.2 Comparison to Global Tin Deposits

To accurately assess the project's potential, it is necessary to benchmark the observed grades against global standards for different types of cassiterite deposits. Cassiterite is the world's only commercially important source of tin, and deposits are broadly classified into two main categories: primary lode deposits and secondary placer deposits.[10]

High-grade primary lode deposits, such as the famous San Rafael mine in Bolivia, can have an average tin grade of 4.7% by weight, with some zones reaching as high as 15%.[11] The Tulu project's grades, while significant, are not indicative of this high-grade lode style of mineralization yet.

However, the vast majority of global tin production comes from placer deposits, particularly in Southeast Asia (Indonesia, Malaysia, Myanmar) and China.[8] These deposits are formed by the concentration of dense cassiterite grains in riverbeds and on shorelines.[6] The average grade for these large alluvial deposits can be as low as 0.01% tin metal.[12] The grades observed in the Tulu pitting program, with multiple samples exceeding 0.2% and reaching a high of 1.96%.

SnO_2 is exceptionally high for a placer deposit. This suggests that the Tulu project has a high-quality resource, which is highly competitive on a global scale within the placer tin market.

CHAPTER FIVE

5.0 CONCLUSIONS, DISCUSSION, AND RECOMMENDATION

5.1 Synthesis of Geochemical and Geological Findings

The exploration program in the Tulu area has been successful in identifying strong indications of cassiterite mineralization. The geological setting is unequivocally that of the Nigerian Younger Granites province, a well-known region for tin production. The geochemical results from both rock and pit samples provide compelling evidence for a two-stage metallogenic process. The presence of anomalous SnO_2 in rock samples points to a primary, disseminated tin source within the bedrock. The widespread and high-grade anomalies identified in the pitting program, particularly the clustering of these anomalies and their vertical persistence to depths exceeding 2 meters, confirm that this primary source has weathered and concentrated into a substantial secondary, placer-style deposit.

5.2 Assessment of the Licensed Area's Exploration Potential

Based on the data analysis, the 40-square-kilometer licensed area in Tulu is considered to have high potential for a commercially viable cassiterite deposit. The observed grades, especially in the pit samples, are a positive indicator that the deposit could be economically significant. The spatial clustering of the anomalies allows for the delineation of priority areas, and the vertical distribution of the mineralization suggests that a deep, robust resource exists, which could support a larger-scale mining operation.

5.3 Identification of Key Geological Controls on Mineralization

The primary geological control on the mineralization is the Jurassic Younger Granite intrusion, which acts as the source rock.[6] The secondary control, and the one most relevant to a potential mining operation, is the physical process of weathering and erosion. This process has led to the formation of residual and alluvial deposits where the heavy and resistant cassiterite grains were naturally concentrated in the regolith and in palaeo-channels. The highest-grade anomalies are found where this process of natural concentration was most effective, creating the clustered zones of interest.

5.4 RECOMMENDATIONS

To effectively advance the exploration project and fully realize its potential, a phased, targeted approach is recommended.

1. **Targeted Infill Pitting and Systematic Trenching:** The existing anomalous clusters require more precise delineation. It is recommended that infill pitting be conducted on a tighter grid (50 x 50 m) within and immediately around the high-grade and anomalous zones. To understand the full vertical and lateral extent of the mineralized horizons, mechanized trenching should be undertaken, particularly in areas where high grades were recorded in the deeper intervals (C and D), in low-lying areas or stream channels, and along.

2. **Heavy Mineral Separation and Metallurgical Test Work:** The current geochemical data are an essential first step, but they represent a total assay rather than a recoverable product. It is recommended that bulk samples from the most promising pits be collected for heavy mineral separation. This process will provide crucial data on the final grade of the cassiterite

concentrate and the potential for recovery, which are essential for conducting a preliminary economic assessment and for designing a future processing flowsheet.

3. **Drilling Program:** In zones of consistently elevated SnO_2 in rock samples, initiate scout core drilling to confirm continuity, grade, and depth extension of primary cassiterite mineralization. The data from previous exploration activities would be used to design a targeted drilling program that systematically tests the deeper regolith and underlying weathered bedrock. This would provide a comprehensive understanding of the resource from the surface down to the primary source.

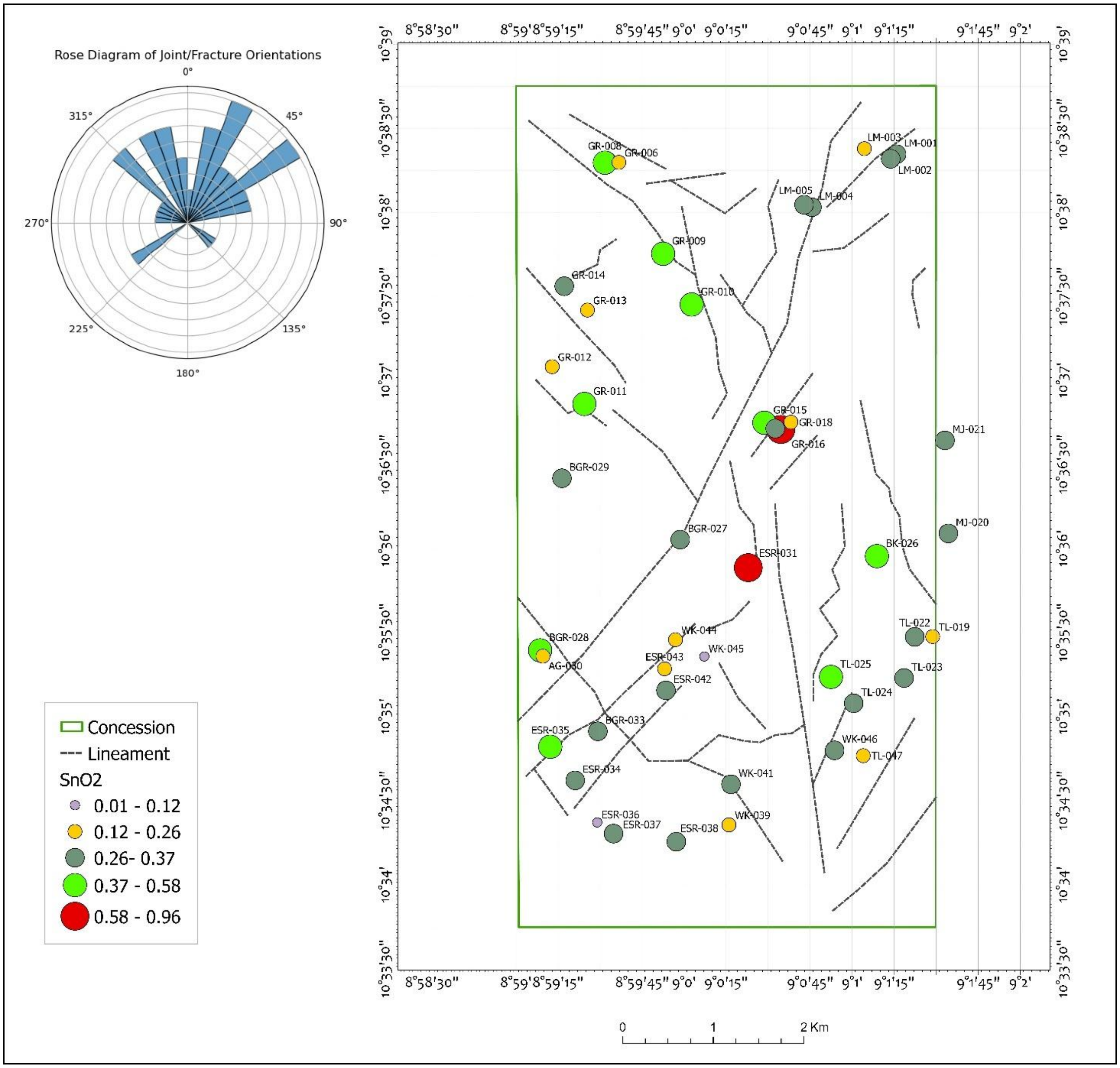

REFERENCES

1. Nigerian Tin Province - Jos Plateau, Sabon Gida Valley, Liruei Lode - PorterGeo Database - Ore Deposit Description, accessed August 22, 2025, Nigerian Tin Province - Jos Plateau, Sabon Gida Valley, Liruei Lode.

2. Mineralization and Geochemical Investigation of Tin Deposit around Maigemu Village, Jos East LGA, North Central Nigeria - IIARD, accessed August 22, 2025, Mineralization and Geochemical Investigation of Tin Deposit around Maigemu Village, Jos East LGA, North Central Nigeria.

3. Genetic Association between Granites and Mineralization at the Gindi Akwati Cassiterite–Sulfide Deposit, North-Central Nigeria: Insights from Mineralogy, Fluid Inclusions, and Sulfur Isotopes - MDPI, accessed August 22, 2025, https://www.mdpi.com/2075-163X/12/6/761

4. Ring Complexes in the Younger Granite Province of Northern Nigeria - Geological Society, London, Memoirs Home, accessed August 22, 2025, Ring Complexes in the Younger Granite Province of Northern Nigeria

5. Geochemical Characteristics of Tin-bearing and Tin-barren Granites, Northern Nigeria - GeoScienceWorld, accessed August 22, 2025, https://pubs.geoscienceworld.org/segweb/economicgeology/article-pdf/75/1/71/3486685/71.pdf

6. Cassiterite - Occurrence, Physical Characteristics and FAQs - Vedantu, accessed August 22, 2025, https://www.vedantu.com/geography/cassiterite

7. Cassiterite | Properties, Formation, Occurrence - Geology Science, accessed August 22, 2025, https://geologyscience.com/minerals/cassiterite/

8. (PDF) Tin in Africa - ResearchGate, accessed August 22, 2025, https://www.researchgate.net/publication/305917893_Tin_in_Africa

9. Tin Ore Production in Nigeria: Mining, Trading, and Export Opportunities Driving Economic Growth, accessed August 22, 2025, https://kelechimineralsltd.com/2025/08/20/tin-ore-production-in-nigeria-mining-trading-and-export-opportunities-driving-economic-growth/

10. Tin Statistics and Information | U.S. Geological Survey - USGS.gov, accessed August 22, 2025, https://www.usgs.gov/centers/national-minerals-information-center/tin-statistics-and-information

11. San Rafael, Peru: geology and structure of the worlds richest tin lode - IIS Windows Server, accessed August 22, 2025, https://app.ingemmet.gob.pe/biblioteca/pdf/MD-38-555.pdf

12. Cassiterite | Oxide Ore, Tin Ore & Ore Mining - Britannica, accessed August 22, 2025, https://www.britannica.com/science/cassiterite

APPENDIX A

Table A.1: Anomalous Pitting Samples ($SnO_2 \geq 0.2\%$) by Location and Depth Interval

hole_id	Lab_id	lat	lon	depth	INTERVAL	SnO_2 (%)
EST-005	DMW-016	10.57427778	9.005666667	2.66	A	0.3
EST-011	DMW-037	10.57563889	9.004861111	2.6	D	0.22
EST-012	DMW-038	10.57591667	9.004777778	1.5	A	0.55
EST-015	DMW-044	10.57255556	9.005416667	2.3	B	0.31
EST-033	DMW-101	10.58197222	8.986138889	2	B	0.2
EST-053	DMW-126	10.58047222	9.002083333	2.2	B	1.96
EST-058	DMW-143	10.57691667	8.985166667	1.7	D	0.74
EST-063	DMW-158	10.57836111	8.984805556	1.7	A	0.52
EST-078	DMW-210	10.58958333	8.987694444	2.3	C	0.32
EST-079	DMW-213	10.59044444	8.988527778	2.6	B	0.38

EST-079	DMW-214	10.59044444	8.988527778	2.6	C	0.3
EST-080	DMW-219	10.59019444	8.988638889	2.3	D	0.28
EST-081	DMW-222	10.59072222	8.988777778	2.5	C	0.48
EST-082	DMW-225	10.59016667	8.989194444	2.8	B	0.3
EST-083	DMW-230	10.59052778	8.989555556	2.3	C	0.23
EST-083	DMW-231	10.59052778	8.989555556	2.3	D	0.23
EST-085	DMW-239	10.576	8.985722222	2.8	D	0.27
ES-005	DMW-266	10.57416667	8.990666667	2.65	A	0.28
ES-006	DMW-270	10.57494444	8.992888889	2.56	A	0.31
BG-003	DMW-385	10.62269444	8.984833333	2.7	A	0.4
BG-003	DMW-386	10.62269444	8.984833333	2.7	B	0.21
BG-003	DMW-387	10.62269444	8.984833333	2.7	C	0.21
BG-005	DMW-391	10.63119444	8.984555556	1.5	C	0.22

ES-035	DMW-364	10.59486111	8.989638889	2.3	D	0.23
BG-015	DMW-418	10.6095	8.996805556	1	A	0.23
BG-025	DMW-448	10.63172222	9.010611111	2.7	D	0.26
BG-027	DMW-456	10.64294444	9.010416667	2.3	D	0.4
BG-029	DMW-462	10.61911111	9.008555556	2.8	C	0.24
BGS-006	DMW-482	10.61255556	9.009416667	1.3	C	0.28
BGS-015	DMW-513	10.62072222	9.015333333	2.6	C	0.24
BGS-015	DMW-514	10.62072222	9.015333333	2.6	D	0.22
BGS-016	DMW-515	10.62177778	9.014722222	2.5	A	0.33
BGS-016	DMW-516	10.62177778	9.014722222	2.5	B	0.26
BGS-016	DMW-517	10.62177778	9.014722222	2.5	C	0.32
BGS-017	DMW-522	10.62244444	9.014944444	2.5	D	0.34
BGS-021	DMW-533	10.62455556	9.01325	2	C	0.51

BGS-023	DMW-538	10.62933333	9.011305556	2.7	A	0.48
BGS-024	DMW-542	10.63077778	9.0105	2.9	B	0.28
BGS-024	DMW-543	10.63077778	9.0105	2.9	C	0.31
BGS-025	DMW-545	10.63227778	9.01225	2.8	A	0.43
BGS-025	DMW-546	10.63227778	9.01225	2.8	B	0.29
BGS-026	DMW-550	10.63447222	9.012416667	2	B	0.27
BGS-027	DMW-554	10.63658333	9.012944444	2.85	B	0.2
BGS-029	DMW-561	10.64180556	9.012972222	3.1	A	0.38
BGS-029	DMW-562	10.64180556	9.012972222	3.1	B	0.33
BGS-029	DMW-563	10.64180556	9.012972222	3.1	C	0.32